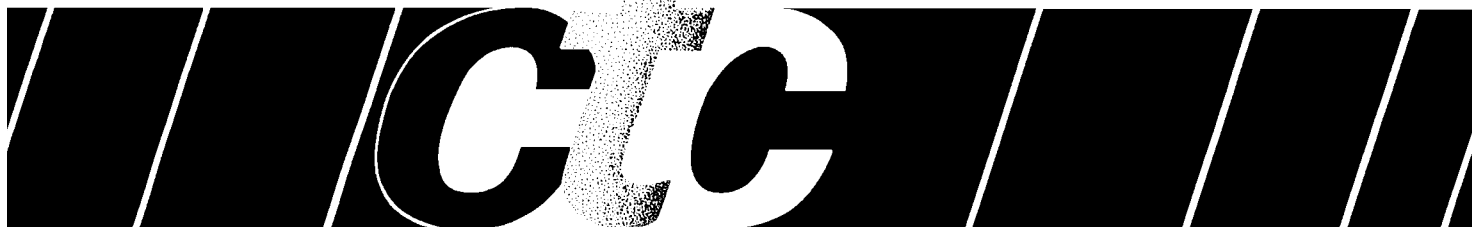




**PILOT-SCALE EVALUATION OF THE POTENTIAL
FOR EMISSIONS OF HAZARDOUS AIR POLLUTANTS
FROM COMBUSTION OF TIRE-DERIVED FUEL**

control *technology center*



EPA REVIEW NOTICE

The research described in this article has been reviewed by the Air and Energy Engineering Research Laboratory, U.S. Environmental Protection Agency, and approved for publication. The contents of this article should not be construed to represent Agency policy nor does mention of trade names or commercial products constitute endorsement or recommendation for use.

**Pilot-Scale Evaluation of the Potential for Emissions of Hazardous Air Pollutants from
Combustion of Tire-Derived Fuel**

Prepared by:

Paul M. Lemieux
U.S. Environmental Protection Agency
Air and Energy Engineering Research Laboratory
Research Triangle Park, NC 27711

Prepared for:

U.S. Environmental Protection Agency
Office of Research and Development
Washington, DC 20460

ABSTRACT

Experiments were conducted in a 73 kW (250,000 Btu/hr) rotary kiln incinerator simulator to examine and characterize emissions from incineration of scrap tire material. The purposes of this project are to: (1) generate a profile of target analytes for full-scale stack sampling efforts, not to generate statistically defensible emission factors for the controlled combustion of scrap tire material; and, (2) where possible, give insight into the technical issues and fundamental phenomena related to controlled combustion of scrap tires. Wire-free crumb rubber sized to < 0.64 cm ($< 1/4$ in) was combusted at two different feed rates, two different temperatures, and at three different kiln oxygen concentrations. Along with continuous emissions monitoring for oxygen (O_2), carbon dioxide (CO_2), carbon monoxide (CO), nitric oxide (NO), sulfur dioxide (SO_2), and total hydrocarbons (THCs), samples were taken to examine volatile and semi-volatile organics, polychlorinated p-dibenzodioxins and dibenzofurans (PCDD/PCDF), and metal aerosols. In addition, a continuous polycyclic aromatic hydrocarbon (PAH) analyzer was used in all the tests. Samples were analyzed with an emphasis on the 189 hazardous air pollutants (HAPs) listed in the 1990 Clean Air Act Amendments (CAAA), but other compounds were also identified where possible.

Results indicate that, if burned in a steady-state mode, TDF combustion will result in very low emissions of CO, THCs, volatile and semi-volatile organics, and PCDD/PCDF. Metal emissions were also very low, with the exception of arsenic (As), lead (Pb), and zinc (Zn). Uncontrolled stack concentrations of As and Pb were 37.16 and 65.96 $\mu\text{g}/\text{Nm}^3$, respectively. Uncontrolled Zn emissions were considerably higher, at 35,465 $\mu\text{g}/\text{Nm}^3$. Results also indicate that organic emissions can increase significantly when TDF is fired in a non-steady mode. The continuous PAH analyzer appeared to track transient operation well, and gave concentration results in the same range as those derived using EPA standard semi-volatile organic sampling methodologies.

Overall, it appears that, with the exception of zinc, potential emissions from TDF combustion are not significantly different from emissions from combustion of conventional fossil fuels, when burned in a well-designed and well-operated combustion device. If unacceptable particulate loading occurs due to zinc emissions, then the emissions would have to be controlled by an appropriate particulate control device.

PREFACE

The Control Technology Center (CTC) was established by EPA's Office of Research and Development (ORD) and Office of Air Quality Planning and Standards (OAQPS) to provide technical assistance to state and local air pollution control agencies. Three levels of assistance can be accessed through the CTC. First, a CTC HOTLINE has been established to provide telephone assistance on matters relating to air pollution control technology. Second, more in-depth engineering assistance can be provided when appropriate. Third, the CTC can provide technical guidance through publication of technical guidance documents, development of personal computer software, and presentation of workshops on control technology matters.

The technical guidance projects, such as this one, focus on topics of national or regional interest that are identified through contact with state and local agencies. In this case, the CTC became interested in examining pollutants emitted from both the controlled and uncontrolled combustion of scrap tires.

Initial tests were conducted to examine the emissions from a simulated tire fire. These simulated open burning tests were completed in 1989 and the final report titled "Characterization of Emissions from the Simulated Open Burning of Scrap Tires" was published as EPA report EPA-600/2-89-054. In 1991, a follow-up to the original open burning study was performed, where the previously sampled organic extracts were subjected to Ames bioassays to determine mutagenic potencies of the extracts, then gas chromatography/mass spectroscopy (GC/MS) analysis to determine which classes of compounds accounted for the mutagenic activity. This report was published as EPA report EPA-600/R-92-127 entitled "Mutagenicity of Emissions from the Simulated Open Burning of Scrap Rubber Tires."

The CTC has also published report EPA-450/3-91-024 entitled "Burning Tires for Fuel and Tire Pyrolysis: Air Implications." This report was a paper study examining the emissions from the use of scrap tires as fuel for processes. Although data on criteria pollutants (CO, SO_x, NO_x, and particulates) were available, little data were available as to the emission of air toxics, including metals and organics. This study was funded in order to help close the data gaps uncovered in the paper study, and to give guidance to state and local air pollution agencies as to which pollutants to measure during sampling tests.

ACKNOWLEDGEMENTS

Portions of this work were conducted under EPA Contract 68-DO-0141 with Acurex Environmental Corporation, and EPA Cooperative Agreement CR-814945-01-0 with University of Arkansas (J.E. Dunn). The author would like to thank: Acurex's Jeff Ryan, who was the Acurex task leader, and coordinated all of the sampling and analytical activities; Marc Calvi, who operated the kiln, tire feeder, and flue gas cleaning system; Mike Bowling, Ed Brown, and Ray Thomas, who operated the sampling equipment; and Hal Buck, who built the tire feeder. Finally, the author would like to thank EPA/AEERL's Frank Briden, who performed the XRD and XRF analyses.

TABLE OF CONTENTS

ABSTRACT	ii
PREFACE	iii
ACKNOWLEDGEMENTS	iv
LIST OF FIGURES.....	vii
LIST OF TABLES	viii
1. INTRODUCTION.....	1
1.1. Scrap Tire Generation Issues.....	1
1.2. Tire Fires	1
1.3. Tire Derived Fuel	2
1.4. Air Emissions from TDF Combustion	3
1.5. Project Objective	3
2. EXPERIMENTAL	5
2.1. Experimental Equipment.....	5
2.1.1. Rotary Kiln Incinerator Simulator.....	5
2.1.2. Tire Derived Fuel (TDF).....	6
2.1.3. Sampling Equipment	7
2.1.4. Data Acquisition System.....	11
2.2. Experimental Approach.....	11
2.2.1. Experimental Design	11
2.2.2. Experimental Procedures.....	12
3. RESULTS.....	16
3.1. Continuous Emission Monitor Samples	16
3.1.1. General Observations	16
3.1.2. Regression Analysis of CO and PAH Data.....	16
3.2. Volatile Organic Samples.....	25
3.3. Semi-Volatile Organic Samples	30
3.3.1. MM5 Sampling Trains	30
3.3.2. Continuous PAH Analyzer.....	30
3.4. PCDD/PCDF Samples.....	31
3.5. Metals Samples.....	31
3.6 Particulate Data	33
3.7. XRD/XRF Results.....	34

3.8. Effect of Transient Operation.....	35
4. CONCLUSIONS.....	43
5. REFERENCES.....	46
APPENDIX A. QA/QC EVALUATION REPORT.....	A-1
A.1. Volatile Organic Samples.....	A-1
A.2. Semi-Volatile Organic Samples	A-1
A.3. PCDD/PCDF Samples.....	A-2
A.4. Metals Samples.....	A-2
A.5. QCER for CEM Data.....	A-3
A.6. General QA Information.....	A-3
APPENDIX B. VOLATILE ORGANIC SAMPLING DATA.....	B-1
APPENDIX C. SEMI-VOLATILE ORGANIC SAMPLING DATA.....	C-1
APPENDIX D. PCDD/PCDF DATA	D-1
APPENDIX E. METALS DATA.....	E-1
APPENDIX F. OTHER DATA.....	F-1

LIST OF FIGURES

Figure 2-1. Rotary kiln incinerator simulator.....	6
Figure 2-2. TDF feeder.....	7
Figure 2-3. Location of sample points.....	9
Figure 2-4. Scatter plot matrix of experimental conditions.....	13
Figure 3-1. Model predictions: emissions of CO as a function of TDF feed rate.....	23
Figure 3-2. Model predictions: emissions of PAH as a function of TDF feed rate.....	24
Figure 3-3. Comparison of VOC emissions between natural gas and TDF combustion.	29
Figure 3-4. Kiln O ₂ and CO ₂ traces during run TB8.	36
Figure 3-5. Stack O ₂ and CO ₂ traces during run TB8.	37
Figure 3-6. PAH analyzer trace during run TB8.....	37
Figure 3-7. Kiln CO traces during run TB8.	38
Figure 3-8. Stack CO traces during run TB8.....	38
Figure 3-9. Kiln O ₂ and CO ₂ traces during run TB9.	40
Figure 3-10. Stack O ₂ and CO ₂ traces during run TB9.	40
Figure 3-11. PAH analyzer trace during run TB9.....	41
Figure 3-12. Kiln CO traces during run TB9.	41
Figure 3-13. Stack CO traces during run TB9.....	42
Figure F-1. CO Model 1.....	F-5
Figure F-2. CO Model 2.....	F-6
Figure F-3. CO Model 3.....	F-6
Figure F-4. PAH Model 1.....	F-7
Figure F-5. PAH Model 2.....	F-8
Figure F-6. PAH Model 3.....	F-8

LIST OF TABLES

Table 1-1. Comparative fuel analysis, by weight.....	2
Table 2-1. Proximate and ultimate analyses of TDF.....	8
Table 2-2. Continuous emission monitors.....	9
Table 2-3. Primary variables of interest.	11
Table 2-4. Run conditions.	14
Table 3-1. CEM data taken at kiln exit.	17
Table 3-2. CEM data taken at SCC exit.	18
Table 3-3. Burner information for kiln and SCC.	19
Table 3-4. Data used for regression analysis.....	20
Table 3-5. Parameters examined in regression analysis.....	21
Table 3-6. Model predictors.	22
Table 3-7. Summary of VOC concentrations (ng/L).....	26
Table 3-8. Estimated emissions of VOCs (ng/J), based on TDF + natural gas.....	27
Table 3-9. Estimated emissions of VOCs (ng/J), based on TDF only.	28
Table 3-10. Stack concentration ($\mu\text{g}/\text{m}^3$) of metals from TDF combustion.	32
Table 3-11. Estimated metals emissions (ng/J) from TDF combustion.	32
Table 3-12. Average emission factors for coal- and oil-fired boilers (ng/J).	33
Table 3-13. Particulate data.....	34
Table 3-14. TDF fly ash composition (wt %) as determined by X-ray fluorescence.....	35
Table 3-15. TDF fly ash composition as determined by X-ray diffraction.....	35
Table A-1. Rotary Kiln Tire Burn CEM Operation Summary.....	A-4
Table A-2. Data quality indicator results for CEM measurements.	A-6
Table F-1. Kiln tire burn runs list.....	F-2
Table F-2. Kiln tire burn sampling summary.....	F-3
Table F-3. Kiln tire burn particulate summary.....	F-4
Table F-4. Residuals from COEMISFAC regression models.	F-5
Table F-5. Residuals (x 1000) from PAHEMISFAC regression models.....	F-7

1. INTRODUCTION

1.1. Scrap Tire Generation Issues

Approximately 240 million vehicle tires are discarded annually in the United States¹. Viable methods for reclamation exist. Some of the attractive options for use of scrap tires include burning, either alone or with another fuel, such as coal, in a variety of energy-intensive processes, such as cement kilns and utility boilers.^{2,3,4} Another potentially attractive option is the use of ground tire material as a supplement to asphalt paving materials. Congress has passed a law, the Intermodal Surface Transportation Efficiency Act of 1991,⁵ which mandates that up to 20 percent of all federally funded roads in the United States include as much as 9 kg (20 lb) of rubber derived from scrap tires per 907 kg (1 ton) of asphalt by 1997. In spite of these efforts, less than 25 percent of the total amount of discarded tires are re-used or re-processed, and the remaining 175 million scrap tires are discarded in landfills, above-ground stockpiles, or illegal dumps. In addition, these reclamation efforts do little to affect the estimated 2 billion tires already present in stockpiles.

Many landfills are refusing to accept tires because they present not only disposal but also health-related problems. After burial, tires often float to the surface and become partially filled with water. Cutting the tire in half or in pieces can reduce this tendency. However, it is very costly to cut or shred tires for landfilling purposes, and in any event, many sites lack the necessary equipment. Steel-belted radials, which comprise the majority of the nation's discarded tires, are particularly difficult to cut and/or shred. Often, they are simply stockpiled or illegally dumped. These stockpiles and dumps can become a breeding ground for many insects, especially mosquitoes, where water collects in the tires and creates an ideal breeding habitat. The introduction and spread of several mosquito species has been directly attributed to the presence of refuse tires.⁶

1.2. Tire Fires

The growing incidence of tire fires creates another potential health hazard. More tire stockpiles and illegal dumps are coming into existence, and with them the occurrence of tire fires. These fires, sometimes started by arson, generate a huge amount of heat, making them extremely difficult to extinguish. Some of these tire fires have continued for months. For example, the Rhinehart tire fire in Winchester, Virginia, burned for nearly 9 months,⁷ exuding large quantities of potentially harmful compounds. Efforts to identify and quantify compounds emitted during tire fires have been successful. Large quantities of volatile organics, such as benzene, semi-volatile organics, such as polycyclic

aromatic hydrocarbons (PAHs), and particulates are released into the atmosphere during tire fires.^{8,9} Emissions from simulated open burning of tires were mutagenic and contained several known carcinogens.^{10,11}

1.3. Tire Derived Fuel

The potential dangers of air emissions from tire fires, though, don't necessarily mean that controlled combustion of scrap tires will produce harmful emissions. Tires can be burned whole, or can be shredded or chipped before burning. Tires that have been processed into smaller pieces are called Tire-Derived Fuel (TDF). There are three main industries that utilize either whole tires or TDF either as a sole fuel or a fuel supplement.³ These industries are:

- Electric utilities that use TDF and whole tires as supplemental feed in power generation. One company is using whole tires as its sole source of fuel in power generation.
- Cement manufacturing companies using tires and TDF to supplement their primary fuel (usually coal) for firing cement kilns. Some of the companies are using tires or TDF directly in the kiln, some are using tires or TDF in the precalciner (prior to the kiln).
- Pulp and paper companies using tires or TDF as supplemental fuel in their waste-wood products boilers.

TDF can be additionally processed to remove the steel belts and the metal bead that surrounds the wheel rim. TDF with the metals removed is termed wire-free, and TDF with the wire remaining is termed wire-in. TDF can be purchased in a variety of size ranges all the way down to < 0.7 cm (< 0.25 in). TDF that is very small is termed crumb rubber. TDF has a higher heating value than coal, and contains about as much sulfur as a medium sulfur coal. Table 1-1 lists a comparative fuel analysis by weight for an average TDF and an average coal.

Table 1-1. Comparative fuel analysis, by weight.¹²

Fuel	Composition (percent)							Heating Value
	Carbon	Hydrogen	Oxygen	Nitrogen	Sulfur	Ash	Moisture	
TDF	83.87	7.09	2.17	0.24	1.23	4.78	0.62	7,428
Coal	73.92	4.85	6.41	1.76	1.59	6.23	5.24	6,396

1.4. Air Emissions from TDF Combustion

The main environmental concern of using whole tires or TDF as supplementary fuel is the potential for increased air emissions. Pollutants of concern include criteria pollutants (CO, SO₂, NO_x, and particulates), metals, and unburned organics. Title III of the 1990 Clean Air Act Amendments (CAAA) includes a list of 189 Hazardous Air Pollutants (HAPs) of concern.¹³ These include volatile organic species such as benzene, polycyclic aromatic hydrocarbons (PAHs) such as benzo(a)pyrene, metal species such as lead, and several individual compounds such as polychlorinated p-dibenzodioxins and polychlorinated dibenzofurans (PCDD/PCDF).

Past field data have shown that, for the most part, emissions of most criteria pollutants are reduced when a fraction of the fuel input is replaced with tires or TDF.^{3,4} This includes SO₂ (which drops if the primary fuel is a high sulfur eastern coal), and NO_x (since tires have very little fuel nitrogen). Uncontrolled emissions of particulates have generally increased slightly. In some cases the ash characteristics changed such that the particulate control devices worked better, and overall particulate emissions were reduced, especially for systems containing electrostatic precipitators (ESPs). Emissions data for other pollutants, however, are either very limited or non-existent.

1.5. Project Objective

A significant data gap exists in the database of HAPs that can be formed from combustion of tires or TDF. This makes it difficult for state and local air pollution agencies to grant air quality permits allowing a facility to supplement its fuel with tires or TDF, since stack sampling is quite expensive, especially when a list of target analytes does not exist. It was for this reason that the CTC funded this particular project. The purposes of this project are to: (1) generate a profile of target analytes for full-scale stack sampling efforts, not to generate statistically defensible emission factors for the controlled combustion of scrap tire material; and, (2) where possible, give insight into the technical issues and fundamental phenomena related to controlled combustion of scrap tires..

There are several issues that are of concern with the use of TDF in combustion devices:

- The effect on products of incomplete combustion (PICs) of the mode of tire feeding (e.g., whole tires vs. shredded tires).
- The potential for the formation of classes of air toxics not normally found in the stacks of the combustion devices while burning conventional fuels.

- The impact of TDF-generated particulate on operation of existing particulate control devices.
- Potential for operational problems due to differences in feed characteristics.
- Potential operational problems due to differences in the residues that are generated.

This project will attempt to address the first two issues listed above. As much as possible, the last three issues will be eliminated from the scope of the project by: 1) utilizing a very uniform feed so as to enable as close to steady-state operation as possible; and 2) to use a grade of TDF that will not generate significant residue.

2. EXPERIMENTAL

2.1. Experimental Equipment

A single laboratory-scale combustor was used to perform all the tests, and the tests were performed in as wide a range of operating conditions as possible, to simulate the process conditions in a variety of combustion units. In addition, it was decided that the scrap tire material be co-fired with natural gas as the primary fuel, rather than coal or wood waste. By using natural gas as the primary fuel, it was hoped that the effect of the TDF could be isolated, rather than adding the additional experimental complications inherent with burning an additional heterogeneous fuel like coal or wood.

2.1.1. Rotary Kiln Incinerator Simulator

The tests were all performed in the EPA's rotary kiln incinerator simulator (RKIS), located in the EPA's Environmental Research Center in Research Triangle Park, NC. The EPA RKIS has been described in detail previously^{14,15}. It has been established that the 73 kW (250,000 Btu/hr) pilot-scale simulator exhibits the salient features of full-scale units with thermal ratings 20 to 40 times larger. The simulator matches the volumetric heat release, gas-phase residence time, and temperature profile of many full-scale hazardous waste incineration units, and yet is flexible enough to allow parametric testing. A schematic drawing of the simulator is presented in Figure 2-1. A small afterburner (43.8 kW; 150,000 Btu/hr) mounted at the base of the secondary combustion chamber served to establish near-isothermal operating conditions throughout the unit. Sample ports are located at various locations.

The effluent from the RKIS is ducted into a dedicated flue gas cleaning system (FGCS) consisting of a 1.1 MW (4,000,000 Btu/hr) afterburner, followed by a spray quench, baghouse, and wet scrubber. The presence of the FGCS enables extremely flexible operation of EPA's research combustors such as the RKIS without venting pollutants into the atmosphere.

Measurements made on the RKIS are not intended to be directly extrapolated to full-scale units. It is, for example, very difficult to scale up some of the important gas-phase mixing phenomena from the simulator, where, for instance, stratification is not a significant factor, to a full scale unit, where stratification is known to be significant¹⁶. In addition, there are significant differences between kilns and other combustion devices, and this study does not address those issues, although some of the information from this study can be applied to other types of combustors, particularly those that burn TDF in the suspension phase. The purpose of the simulator is to individually examine the fundamental phenomena that occur in full-scale units, and to gain an understanding of the qualitative trends that

would be found in a full-scale rotary kiln. In no way should it be inferred that the concentrations of pollutants from this apparatus would be the same as those from full-scale units.

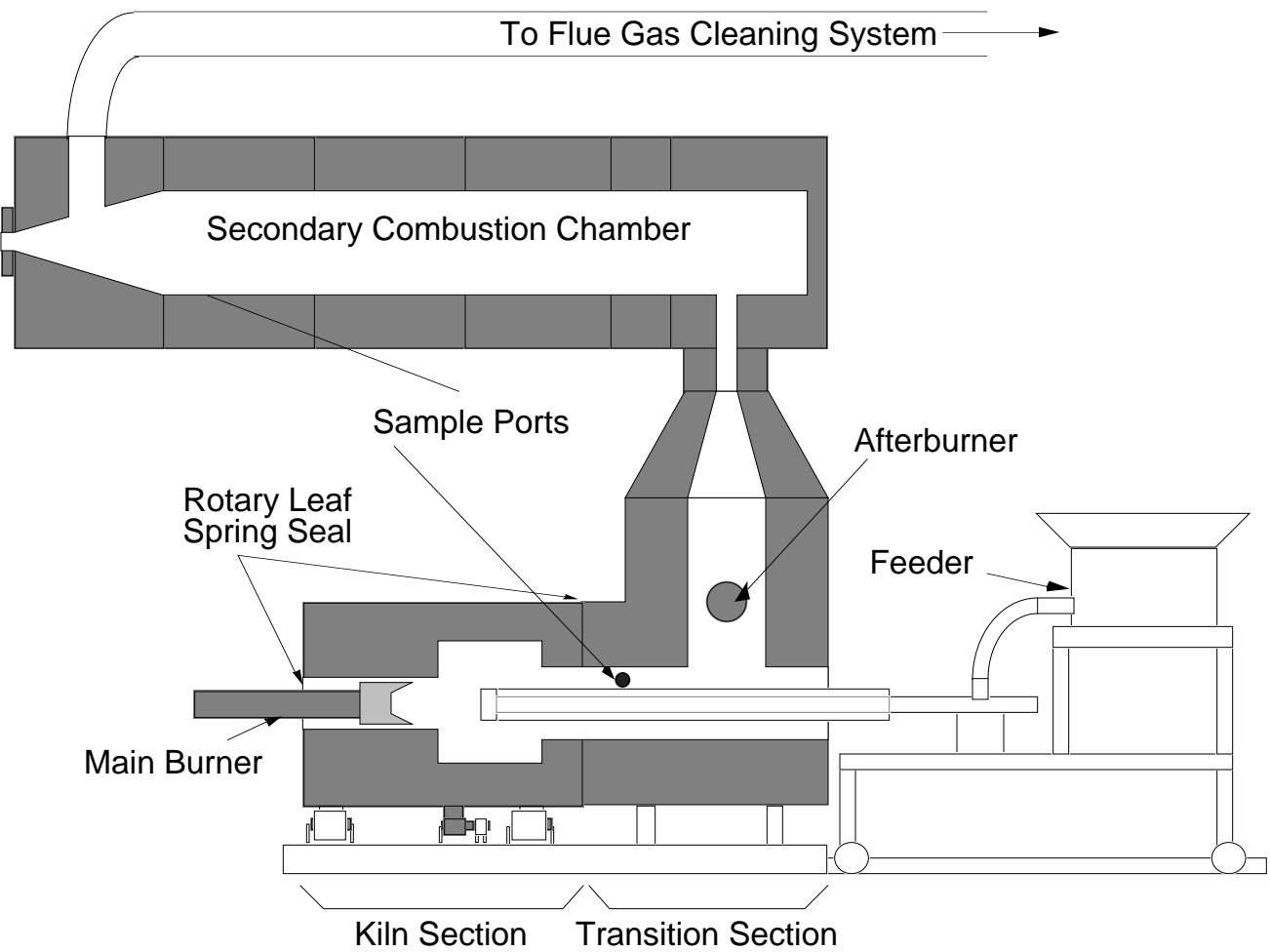


Figure 2-1. Rotary kiln incinerator simulator.

2.1.2. Tire Derived Fuel (TDF)

TDF, consisting of wire-free crumb rubber, sized < 0.64 cm (< 0.25 in), was introduced into the kiln via a vibrating feeder. This feeder (shown in Figure 2-2) consists of an AccuRate screw feeder (model # 604), which dropped a controlled amount of tire material into a stainless steel tube connected to a vibrator (Dyna-Slide model # S0496). The stainless steel tube was inserted through a water jacketed annular tube so that the outlet to the feeder tube lied over the centerline of the kiln's internal recess chamber. Industrial grade nitrogen (N_2) was purged through the feeder to cool and provide an inert atmosphere to prevent the in-transit TDF from combusting or pyrolyzing. The feeder enabled feed rates ranging from 0 to 2 kg/hr to be continuously fed into the RKIS.

The TDF material underwent a proximate and ultimate analysis, as well as an analysis for metals, the results of which are tabulated in Table 2-1. TDF contains significant amounts of zinc (Zn), since Zn is extensively used in the tire manufacturing process.

2.1.3. Sampling Equipment

Gases were monitored with continuous emission monitors (CEMs) to measure oxygen (O₂), carbon dioxide (CO₂), carbon monoxide (CO), nitric oxide (NO), and total hydrocarbons (THC) both before and after the secondary combustion chamber (SCC), as well as sulfur dioxide (SO₂) at the SCC exit. In addition, a continuous photoelectric polycyclic aromatic hydrocarbon (PAH) analyzer sampled the gases at the stack exit. Table 2-2 lists the gas analyzers used in this study. Figure 2-3 illustrates the sampling locations used for this study.

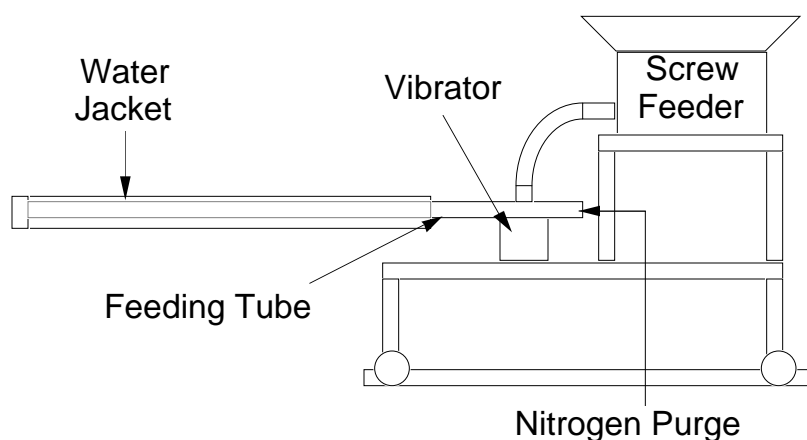


Figure 2-2. TDF feeder.

Table 2-1. Proximate and ultimate analyses of TDF.

Ultimate Analysis	
Moisture	0.84 %
Carbon	76.02 %
Hydrogen	7.23 %
Kjeldahl Nitrogen	0.34 %
Sulfur	1.75 %
Total Halogens (calculated as chlorine)	0.31 %
Ash	7.20 %
Proximate Analysis	
Moisture	0.84 %
Volatile Matter	65.52 %
Ash	7.20 %
Fixed Carbon	26.44 %
Metals	
Cadmium	<5 ppm
Chromium	<5 ppm
Iron	295 ppm
Lead	51 ppm
Zinc	2.14 %
Heating Value	7,666 kJ/kg

Table 2-2. Continuous emission monitors

Analyte	Method	Analyzer
O ₂	paramagnetic	Beckman 755, 755R
CO	non-dispersive infrared	Beckman 864
		Horiba PIR-2000
CO ₂	non-dispersive infrared	Beckman 864, 880
		Horiba PIR-2000
NO	chemiluminescent	TECO 10A
SO ₂ *	ultraviolet	Teledyne 611DAMC-X
		TECO 48
		Anacon 207
THC	flame ionization	Beckman 402
PAH	photoelectric	EcoChem PAS 1000e

* the SO₂ analyzers had problems; three different analyzers were tried before reliable operation was attained.

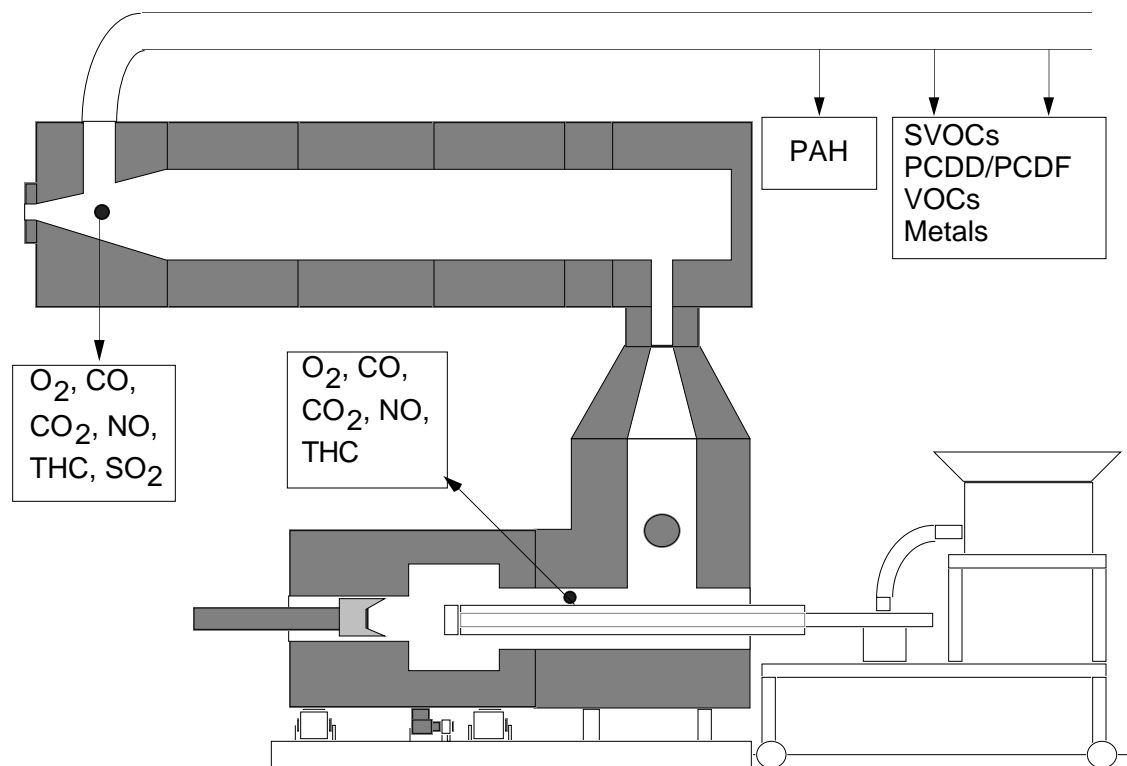


Figure 2-3. Location of sample points.

VOCs were collected by a Volatile Organic Sampling Train (VOST) system¹⁷ located as shown in Figure 2-3. For each run where VOCs were measured, VOST tubes were taken sequentially in triplicate (to judge reproducibility) and each VOST tube was analyzed separately. VOST samples were analyzed using a gas chromatograph/mass spectrometer (GC/MS) system to determine the concentration of 59 separate VOCs, 38 of which are listed under Title III of the CAAAs^{18,19}. The majority of these compounds were either very near to or below the detection limits of the equipment. The high frequency of concentrations below the detection limit (BDL) requires that the average concentrations not be reported as precise values. Concentrations below the equipment detection limits should not arbitrarily be assigned the value of zero, nor should they be given the value of the detection limit. Rather, the actual value likely lies between the two extremes. For the purposes of this study, however, if a compound was detected at above the detection limit in one or more of the VOST tubes, then, for averaging purposes, the detection limits were used as the concentrations for the other VOST tubes. All VOC data are presented in Appendix B, however, if a more detailed treatment is required.

Semi-volatile organics and bulk particulate were collected by isokinetic sampling protocols with a Modified Method 5 (MM5) train²⁰ located as shown in Figure 2-3. The MM5 procedure did not result in multiple samples for each run, as was the case with VOST. Rather, a single integrated sample over the course of the entire run was produced. Collected samples were analyzed using approved analysis procedures²¹ for 95 semivolatile organic compounds, 61 of which are listed as hazardous under Title III¹³. Of the 61 listed compounds, 20 are PAHs.

Metal aerosols were collected by the Multiple Metals Train (MMT),²² with the exception that the potassium permanganate (KMnO₄) impinger solution (used for collection of mercury (Hg) from the sample) was omitted. No literature could be found that reported the presence of mercury in tires, and due to the limited funding for this project, mercury analysis was omitted, which made it unnecessary to configure the sampling train for mercury sampling.

PCDD and PCDF were sampled using the MM5 train with the protocols laid out in EPA Method 23²³ and analyzed by high resolution gas chromatography/low resolution mass spectrometry (HRGC/LRMS), using a Hewlett-Packard 5890/5970 Gas Chromatography/Mass Selective Detector (GC/MSD) system and methods that are slight adaptations to EPA Method 23 and RCRA Method 8280²⁴. Isotopically labeled internal standards for each congener class are incorporated during the extraction and cleanup phases of the analytical procedures to enhance analytical accuracy. For the GC/MSD analyses, the procedures differed from RCRA Method 8280 only in the number of labeled congeners used to calculate

recoveries, i.e., congeners containing the 2,3,7,8 substitution positions are avoided as a safety precaution. An internal standard was used that consisted of a $^{13}\text{C}_{12}$ -labeled congener from each tetra-octa PCDD/PCDF (except for octa-CDF). The recovery standard $^{6}\text{C}_{12}$ -labeled TCDD is added before injection on the GC. The recovery must be within 40 and 120 percent to be acceptable.

2.1.4. Data Acquisition System

All CEMs and thermocouples are connected to a microcomputer-based data acquisition system which allows on-screen visualization of data, conversion of data to engineering units, and date/time stamping of data for later reference. This system, run on an Apple Macintosh IIcx, uses the Strawberry Tree Workbench Mac software²⁵. All files are output in tab-delimited ASCII format for later manipulation. Data were logged to disk every 10 sec. for all input channels.

2.2. Experimental Approach

2.2.1. Experimental Design

A response-surface experimental design²⁶ was used to reduce the number of tests required. The primary variables of interest (both dependent and independent) are listed in Table 2-3. Note also that some variables are functions of other variables, for example, the feed rate of tires and the gas temperature inherently cannot be totally separated from the oxygen concentration.

Table 2-3. Primary variables of interest.

Independent	
	1) Kiln exit temperature
	2) Kiln O ₂ concentration
	3) Tire feed rate
	4) Feed mode (batch vs. continuous)
Dependent	
	1) CO emissions
	2) particulate emissions
	3) metals emissions
	4) PIC emissions (THC, PAH, volatile organics, semi-volatile organics, and PCDD/PCDF)

The test conditions were achieved by varying kiln firing rate, combustion air flow rate, and tire feed rate. Figure 2-4 illustrates a scatter plot the experimental design points achieved with respect to the independent variables No. 1 through 3. For the response-surface methodology to be valid, data must be available over the desired range of values of the independent variables. Variations in independent variable No. 4 (mode of TDF feeding) were achieved by performing two additional tests: one test where the tires were introduced in 300 g batches spaced 10 min. apart; and one test where the kiln air flow rate was ramped up and down every 10 minutes to change the kiln oxygen concentration. Table 2-4 tabulates the run numbers and their respective kiln operating conditions.

2.2.2. Experimental Procedures

Since the feeder is water-cooled, it was removed when experiments were not being performed so that the loss of cooling water would not lead to failure of the water jacket and thermal shock to the kiln's refractory from having water being poured on the refractory once cooling water flow was re-established. Another side effect of the feeder being water cooled was that it provided a heat sink for the hot kiln gases, resulting in cooler operation than is normally found at the identical fuel and air settings without the feeder present. For this reason, the kiln was run at a higher firing rate with the feeder installed so that temperatures could be maintained.

With the exceptions of Runs No. TB8 and TB9, the following test protocol was used. The kiln was allowed to come to thermal equilibrium at a given temperature by setting the main burner and afterburner to the desired air and fuel flow rates. The main flame was then extinguished, and the tire feeder was weighed and installed. Once the feeder was installed, the main flame was re-lit, and the desired run settings were achieved. On blank runs (with 0 kg/hr TDF feed rate), the feeder was installed as well, and the nitrogen purge was maintained; however, no TDF was fed. The desired TDF feed rate was dialed into the feeder control, and the system was allowed to stabilize. Due to the time it took for the TDF to travel down the feeder tube, it took approximately 30 minutes from the initiation of TDF feed before the system stabilized. Once steady-state was achieved, sampling was initiated. For runs where no organic or metals sampling was to be performed, CEMs were operated for 10 minutes, with the CEM results being averaged over the 10 minute run time. For runs where organic or metals sampling was performed, sample duration was determined by the requirements of the sampling methodology being used, which was determined by the requirements that a given volume be pulled through the sample train at isokinetic conditions.

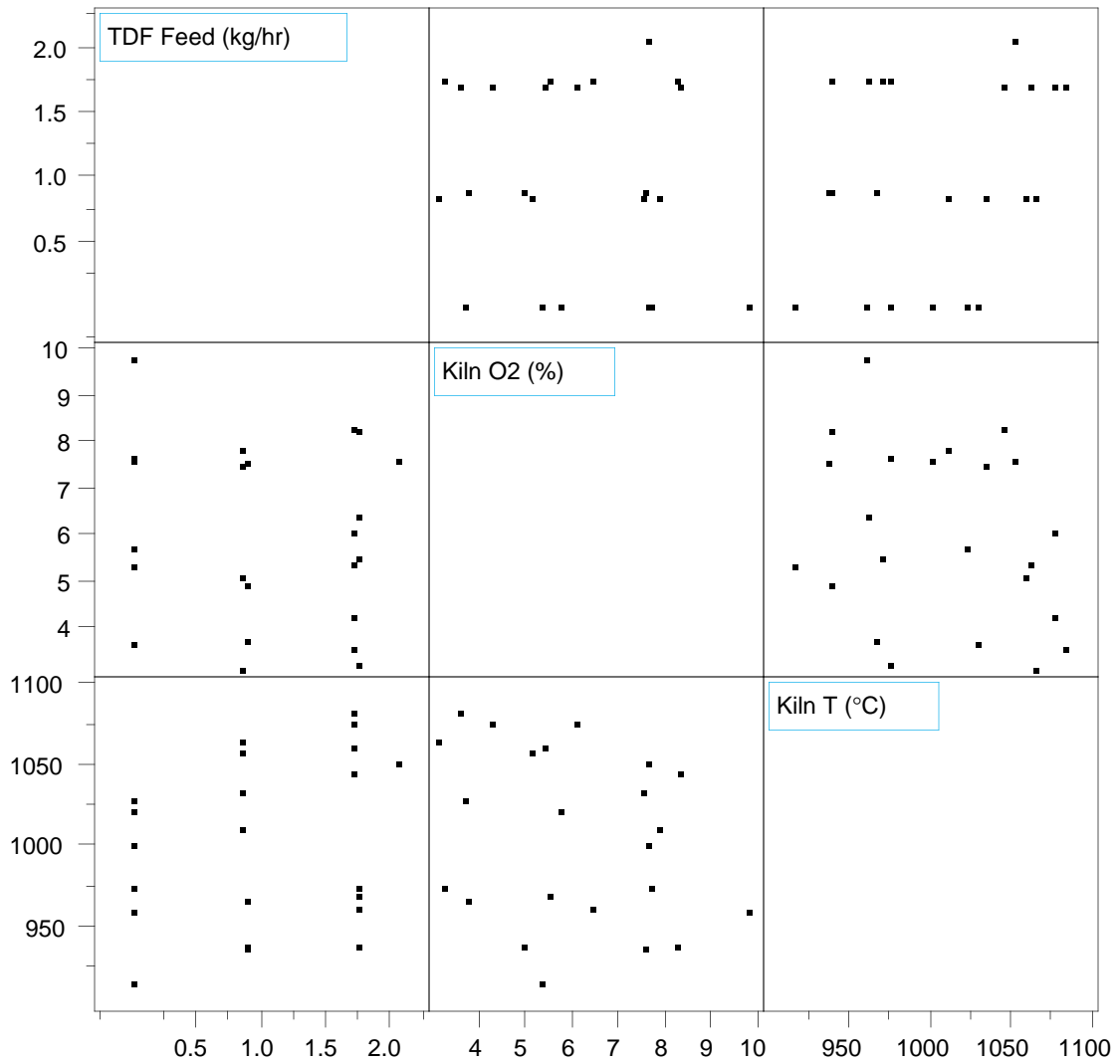


Figure 2-4. Scatter plot matrix of experimental conditions.

Table 2-4. Run conditions.

Run	TDF Feed Rate (kg/hr)	% Total Fuel as TDF	Kiln O ₂ (%)	Kiln T (°C)	SCC T (°C)	Other Samples [‡]
TB1*	0.74	7.23	8.28	1009	896	V
TB2*	1.95	16.95	7.17	1034	924	S
TB3*	2.02	17.14	7.35	1045	962	V, S
TB4*	1.81	15.50	8.51	1030	964	S
TB5*	0.00	0.00	9.23	990	952	V, S
TB6	2.05	17.30	7.64	1052	979	D, M
TB7	0.00	0.00	9.82	959	896	D, M
TB8 ⁺	2.31	19.18	6.45	1059	962	V, S
TB9 ⁺	1.74	14.97	8.38	1042	918	V, S
TB10	0.00	0.00	7.66	975	824	
TB11	0.00	0.00	3.68	1029	830	
TB12	0.00	0.00	5.71	1022	842	
TB13	0.00	0.00	7.62	1001	857	
TB14	0.85	7.80	7.85	1011	884	
TB15	0.85	7.80	3.10	1065	875	
TB16	0.85	7.80	5.07	1058	886	
TB17	0.85	7.80	7.53	1033	901	
TB18	1.70	14.54	5.40	1061	909	
TB19	1.70	14.54	3.55	1082	910	
TB20	1.70	14.54	8.32	1045	927	
TB21	1.70	14.54	4.24	1077	925	
TB22	1.70	14.54	6.06	1077	931	
TB23	0.00	0.00	5.33	916	860	
TB24	0.88	11.99	4.91	939	871	
TB25	0.88	11.99	7.59	937	879	
TB26	0.88	11.99	3.70	966	872	
TB27	1.75	21.41	3.18	975	884	
TB28	1.75	21.41	6.39	962	887	
TB29	1.75	21.41	8.23	938	889	
TB30	1.75	21.41	5.49	970	887	

[‡] V = volatile organics; S = semi-volatile organics; M = metals; D = dioxins

* electrical noise problems on the CEMs.

+ non-continuous feed tests

After sampling was completed, the kiln flame was extinguished, the feeder removed and re-weighed, and the kiln re-lit. Mass feed rates were calculated based on the weight difference between the feeder at the beginning and at the end of the day (including the mass of TDF added during the day to keep the feeder full). Feed rates were adjusted by an estimate of the amount of TDF that was found to build up in the feeder tube during calibration runs.

For Run No. TB8, the procedure above was performed, with the additional operation of changing the volumetric flow rate of the main burner combustion air back and forth between 140 Nm³/hr (5000 scfh) and 112 Nm³/hr (4000 scfh) every 10 minutes to simulate transient operation. For Run No. TB9, an attempt was made to simulate the transient operation that might occur in a system feeding whole tires at periodic intervals rather than feeding TDF continuously. This test was performed by loading 300 g of TDF into a 0.9 L (1 qt) cardboard container and feeding the containers into the kiln every 10 min, by using a manual charging basket/ramrod feeder as described previously^{12,13}. Note that isokineticity was not precisely maintained during the transient tests, due to the constantly changing stack gas volumes.

Particulate samples that were found deposited in the sight ports on the TDF feeder were subjected to X-Ray Diffraction (XRD) and X-Ray Fluorescence (XRF) analysis to determine composition and speciation of the metals in the particulate.

3. RESULTS

3.1. Continuous Emission Monitor Samples

3.1.1. General Observations

All CEM data were averaged over the course of the run to yield a single number. The CEMs were giving extremely noisy responses in runs No. TB1 through TB5. This noise problem was traced to the electrical circuits, and was eliminated in all runs after TB5. For this reason, validity of average responses from many of the CEMs (especially CO, SO₂, PAH) are questionable for runs No. TB1 through TB5. Table 3-1 lists the average values from the CEMs taken at the kiln exit sample port. Table 3-2 lists the average values from the CEMs taken at the exit of the secondary combustion chamber, with the exception of the PAH data, which were taken at the duct sample port shown in Figure 2-3. Other data of importance, such as kiln and afterburner firing rates, flow rates of the gaseous effluent leaving the kiln and secondary combustion chamber (SCC), and relevant temperatures, are listed in Table 3-3. In addition, the NO and SO₂ analyzers were not always behaving as per required Quality Assurance guidelines, due to excessive drift of the responses between initial pre-run calibration and post-run Quality Control checks.

Of particular note is the fact that THC measurements (both at the kiln exit and the SCC exit) were, for all practical purposes (except for Run No. TB9, which will be discussed later), in the range from 0 to 5 ppm, which is of the same order of magnitude as the resolution of the THC analyzer. In addition, CO measurements were always (except, again, in the case of Run No. TB9) less than 100 ppm, indicating that "good" combustion conditions were occurring. This is likely from the steady-state feeding of the TDF, which burned quite well when fed at a constant rate. Also note that for every run performed at steady-state conditions, stack CO measurements were on the order of 20 ppm; even those where no TDF was being burned. This observation would indicate that the SCC was successfully burning residual CO from the kiln down to a lower limit of approximately 20 ppm. Emissions below this limit were not attainable from the apparatus given the fact that the afterburner conditions were fixed for the entire set of runs.

3.1.2. Regression Analysis of CO and PAH Data

Based on these initial observations, it was decided that THC, both at the kiln exit and SCC exit, as well as CO at the SCC exit, would not be appropriate variables to examine with regards to the effect of TDF on emissions. Data were prepared for a regression analysis, with the dependent variables being the

emission rates of CO at the kiln exit; and the emission rate of PAH at the stack exit. Data used for the regression analysis are listed in Table 3-4. Note that only the steady-state tests were used in the regression analysis.

Table 3-1. CEM data taken at kiln exit.

Run	O ₂ (%)	CO ₂ (%)	CO (ppm)	NO (ppm)	THC (ppm)
TB1*	8.28	7.33	33	52	3
TB2*	7.17	7.45	36	73	3
TB3*	7.35	7.70	16	58	0
TB4*	8.51	7.14	31	54	1
TB5*	9.23	6.31	44	39	0
TB6	7.64	7.77	20	55	1
TB7	9.82	5.85	17	32	2
TB8+	6.45	8.38	30	60	1
TB9+	8.38	7.32	700	53	43
TB10	7.66	7.09	30	39	-1
TB11	3.68	9.34	38	53	0
TB12	5.71	8.22	36	47	1
TB13	7.62	7.15	35	40	0
TB14	7.85	7.25	35	46	1
TB15	3.10	9.97	42	62	2
TB16	5.07	8.86	40	57	1
TB17	7.53	7.43	35	50	1
TB18	5.40	8.92	44	62	1
TB19	3.55	10.00	48	64	1
TB20	8.32	7.35	41	54	1
TB21	4.24	9.59	47	64	1
TB22	6.06	8.71	43	62	1
TB23	5.33	8.08	28	56	0
TB24	4.91	9.03	50	66	1
TB25	7.59	7.55	45	64	1
TB26	3.70	9.71	51	65	2
TB27	3.18	10.24	59	68	1
TB28	6.39	8.54	54	66	2
TB29	8.23	7.39	54	58	1
TB30	5.49	8.94	53	68	1

* electrical noise problems on the CEMs.

+ non-continuous feed tests

Table 3-2. CEM data taken at SCC exit.

Run	O ₂ (%)	CO ₂ (%)	CO (ppm)	NO (ppm)	THC (ppm)	SO ₂ (ppm)	PAH (ng/m ³)
TB1*	7.59	8.62	16	49	-2	12	1437
TB2*	5.43	9.44	14	64	-1	81	2278
TB3*	5.62	9.62	12	48	-2	59	2284
TB4*	6.78	9.07	20	62	2	67	3289
TB5*	7.50	8.44	16	52	1	14	1941
TB6	6.06	9.45	15	60	1	51	982
TB7	8.10	7.80	9	42	2	35	429
TB8+	5.20	10.07	18	58	1	76	1957
TB9+	8.85	8.11	70	46	6	26	214000
TB10	6.23	8.86	13	28	0	.	410
TB11	2.82	10.77	17	36	0	.	630
TB12	4.49	9.94	16	35	-1	.	404
TB13	6.17	9.01	16	30	0	.	426
TB14	6.60	8.99	16	35	0	42	767
TB15	2.48	11.18	20	46	0	.	1553
TB16	4.07	10.35	19	44	0	103	1313
TB17	6.28	9.15	17	41	0	106	702
TB18	4.30	10.46	19	50	0	.	1939
TB19	2.61	11.33	20	50	0	96	2364
TB20	7.12	9.00	18	45	0	82	1474
TB21	3.20	11.01	20	50	0	74	1937
TB22	5.01	10.18	20	50	0	78	1734
TB23	4.11	9.94	13	32	-1	7	925
TB24	4.40	10.30	19	36	-1	26	1581
TB25	6.85	9.02	18	37	-1	22	618
TB26	3.68	10.60	20	36	0	42	1550
TB27	3.47	10.83	20	37	0	108	1787
TB28	5.97	9.68	20	39	0	106	1632
TB29	7.36	8.88	20	36	0	100	1130
TB30	5.39	9.93	19	37	0	84	1551

* electrical noise problems on the CEMs.

+ non-continuous feed tests

. analyzer non-operational

Table 3-3. Burner information for kiln and SCC.

Run	Main Burner Air Flow Rate (Nm ³ /hr)	Main Burner Fuel Flow Rate (Nm ³ /hr)	Main Burner Firing Rate (kW)	SCC Burner Air Flow Rate (Nm ³ /hr)	SCC Burner Fuel Flow Rate (Nm ³ /hr)	SCC Firing Rate (kW)	TDF Firing Rate (kW)	Kiln Gas Flow Rate (Nm ³ /hr)	SCC Gas Flow Rate (Nm ³ /hr)
TB1	146.82	8.64	91.07	36.9	3.43	37.23	9.28	160.36	196.32
TB2	161.55	8.75	92.30	36.9	3.43	37.23	21.96	171.75	208.84
TB3	158.55	8.92	94.02	36.9	3.43	37.23	22.50	148.97	208.92
TB4	165.48	9.03	95.06	36.9	3.43	37.23	20.50	147.56	215.89
TB5	144.59	9.03	95.18	36.9	3.43	37.23	0.00	136.83	194.20
TB6	165.29	8.95	94.22	36.9	3.43	37.23	22.74	172.33	215.69
TB7	152.74	8.98	94.63	36.9	3.43	37.23	0.00	148.12	202.29
TB8	153.00	8.92	93.94	36.9	3.43	37.23	25.16	137.38	203.41
TB9	169.79	9.03	95.02	36.9	3.43	37.23	19.80	177.24	220.16
TB10	135.27	9.15	96.28	36.9	3.43	37.23	0.00	139.77	184.97
TB11	107.60	9.15	96.28	36.9	3.43	37.23	0.00	117.81	157.06
TB12	120.15	9.15	96.28	36.9	3.43	37.23	0.00	128.22	169.78
TB13	134.85	9.15	96.28	36.9	3.43	37.23	0.00	139.77	184.53
TB14	148.18	9.15	96.28	36.9	3.43	37.23	10.42	140.15	197.35
TB15	115.51	9.15	96.28	36.9	3.43	37.23	10.42	118.12	164.46
TB16	127.37	9.15	96.28	36.9	3.43	37.23	10.42	128.60	176.53
TB17	145.80	9.15	96.28	36.9	3.43	37.23	10.42	140.15	194.99
TB18	142.24	9.15	96.28	36.9	3.43	37.23	19.41	140.54	191.09
TB19	129.86	9.15	96.28	36.9	3.43	37.23	19.41	134.86	178.71
TB20	165.94	9.15	96.28	36.9	3.43	37.23	19.41	151.88	214.73
TB21	134.62	9.15	96.28	36.9	3.43	37.23	19.41	140.54	183.47
TB22	146.03	9.15	96.28	36.9	3.43	37.23	19.41	140.54	194.85
TB23	78.32	5.89	62.06	36.9	3.43	37.23	0.00	89.90	124.18
TB24	86.51	5.89	62.06	36.9	3.43	37.23	11.90	90.29	132.35
TB25	98.29	5.89	62.06	36.9	3.43	37.23	11.90	90.29	144.13
TB26	81.61	5.89	62.06	36.9	3.43	37.23	11.90	90.29	127.43
TB27	91.10	5.89	62.06	36.9	3.43	37.23	21.26	90.68	136.89
TB28	106.73	5.89	62.06	36.9	3.43	37.23	21.26	105.13	152.69
TB29	120.63	5.89	62.06	36.9	3.43	37.23	21.26	119.84	166.76
TB30	102.51	5.89	62.06	36.9	3.43	37.23	21.26	105.07	148.47

Table 3-4. Data used for regression analysis.

Run	CO emission rate (g/hr)	Estimated CO emissions (ng/J)	PAH emission rate (mg/hr)	Estimated PAH emissions (ng/J)
TB1*	5.33	16.26	0.28	8.54E-04
TB2*	6.34	19.08	0.48	1.44E-03
TB3*	2.36	6.97	0.48	1.42E-03
TB4*	4.51	13.18	0.71	2.07E-03
TB5*	5.99	17.48	0.38	1.11E-03
TB6	3.56	10.50	0.21	6.19E-04
TB7	2.50	7.34	0.09	2.64E-04
TB8+	4.01	11.86	0.40	1.18E-03
TB9+	125.96	368.26	47.11	1.38E-01
TB10	4.13	11.92	0.08	2.31E-04
TB11	4.32	12.46	0.10	2.89E-04
TB12	4.45	12.84	0.07	2.02E-04
TB13	4.82	13.91	0.08	2.31E-04
TB14	4.85	13.99	0.15	4.33E-04
TB15	4.77	13.76	0.26	7.50E-04
TB16	4.98	14.37	0.23	6.64E-04
TB17	4.84	13.97	0.14	4.04E-04
TB18	6.00	17.31	0.37	1.07E-03
TB19	6.27	18.09	0.42	1.21E-03
TB20	6.20	17.89	0.32	9.23E-04
TB21	6.44	18.58	0.36	1.04E-03
TB22	5.98	17.25	0.34	9.81E-04
TB23	2.47	11.06	0.11	4.92E-04
TB24	4.48	20.05	0.21	9.40E-04
TB25	3.99	17.86	0.09	4.03E-04
TB26	4.48	20.05	0.20	8.95E-04
TB27	5.18	23.19	0.24	1.07E-03
TB28	5.62	25.16	0.25	1.12E-03
TB29	6.53	29.23	0.19	8.50E-04
TB30	5.52	24.71	0.23	1.03E-03

* electrical noise problems on the CEMs.

+ non-continuous feed tests - not used in regression analysis

The regression analysis was performed using the SAS statistical software package. Parameters examined in the regression analysis (and their definitions) are listed in Table 3-5. The RSQUARE option in SAS procedure REG was used to obtain the best fitting models using R**2 (multiple R-squared) as a selection criterion. An attempt was made to model the variation in each of the response variables taken in each of three forms, namely its actual value, its logarithm, and its reciprocal. The available predictor set initially consisted of KFEEDPCT, KILNT, KILNO2, and either KILNGAS or KILNFUEL, where use of each form of the latter was used separately. In addition, all squares and two-factor products of the four predictors were made available for selection. Once the highest R² models

were obtained in this way, then reciprocals and logarithms of KILNO2, KILNT, and either KILNGAS or KILNFUEL were made available for switches among the predictors, using the MAXR option, with the goal of obtaining an improved fit (higher R²) while maintaining the original number of predictors. The ultimate criterion for choosing a final model was that all predictors in the model were significant, and no other predictor could be added from within the excluded list of predictors which attained significance when added to the model. A significance level of $p \leq 0.01$, indicating the probability level that the partial effect of a predictor is significantly different from zero, was chosen as the acceptance criterion.

Table 3-5. Parameters examined in regression analysis.

Parameter	Definition
Dependent variables	
KFEEDPCT	% of kiln fuel as TDF
KILNO2	kiln O ₂ (%)
KILNT	kiln T (°C)
KILNAIR	kiln combustion air (Nm ³ /hr)
KILNFUEL	kiln natural gas fuel (Nm ³ /hr)
KILNGAS	kiln exhaust flow rate (Nm ³ /hr)
Response variables	
COEMISFAC	CO emissions (ng/J total heat input)
PAHEMISFAC	PAH emissions (ng/J total heat input)

Table 3-6 lists the model predictors for the regression model. By multiplying the predictor by the value of the coefficient and summing this total for all coefficients, the predicted value of the result can be derived. Note that certain models require this total must be exponentiated after being calculated. The simplest model for COEMISFAC involves only KFEEDPCT and KILNFUEL. This is attributed to the fact that COEMISFAC was so reactive every time KILNFUEL underwent a change. The list of KILNGAS values are relatively noisy by comparison. Model-1 and Model-2 apply almost identically to the prediction of ln(COEMISFAC). Estimated regression coefficients (R²) are shown for each model. p-values associated with tests of the partial effects of each of the terms in the models were universally ≤ 0.0001 . The best model based on KILNGAS rather than KILNFUEL provides a direct prediction of COEMISFAC (without exponentiation) and is characterized below in terms of its estimated coefficients as Model-3. Again, p-values associated with tests of the partial effects of the individual terms in the model were all ≤ 0.0001 . This model involves three of the four pre-selected predictor variables, KILNO2 having no significant effect in the model. Furthermore, these predictors are specific to the untransformed response, COEMISFAC. By contrast, R² drops to 0.9005 when the same predictors are used to predict ln(COEMISFAC). The single difficulty with use of either Model-1 or Model-2, is that they both seriously underestimate the observed response for Run TB29.

Table 3-6. Model predictors.

Predictor	Model-1*	Model-2*	Model-3
COEMISFAC	R2 = 0.95189	R2 = 0.95193	R2 = 0.9374
intercept	55.69512	-417.507	26.888
KFEEDPCT	0.019876	0.0198886	0.383806
KILNFUEL	-14.822410	•	•
KILNFUEL^2	0.984505	•	•
ln(KILNFUEL)	•	139.523	•
1/KILNFUEL	•	1016.867	•
KILNT^2	•	•	-8.706E-5
KILNGAS^2	•	•	-4.93807E-3
KILNT x KILNGAS	•	•	1.210081E-3
PAHEMISFAC	R2 = 0.9206	R2 = 0.9778	R2 = 0.9410
Intercept	3.7475E+00	7.1829E+01	-1.3428E-02
KFEEDPCT	•	-2.8505E-01	-2.2349E-04
KILNO2	•	•	-3.0193E-04
KILNT	•	-4.4491E-02	•
KILNGAS	•	-5.1808E-01	•
KFEEDPCT^2	-1.5930E-03	-1.4292E-03	•
KILNO2*KFEEDPCT	-1.0619E-02	•	•
KILNT*KFEEDPCT	•	3.7836E-04	2.5232E-07
KILNT*KILNO2	•	-1.0769E-03	•
KILNGAS*KFEEDPCT	1.3552E-03	•	•
KILNGAS*KILNO2	•	8.1143E-03	2.0806E-06
KILNGAS*KILNT	-5.5331E-05	3.4782E-04	6.1586E-08
KILNGAS^2	•	•	-3.0212E-07
1/KILNGAS	-6.2066E+02	-1.7409E+03	•
1/KILNT	•	•	1.0991E+01

* - model requires exponentiation of result to convert to predicted COEMISFAC and PAHEMISFAC.

A complete list of the residuals, i.e., [observed - fitted], for all 3 models can be found in Table F-2 in Appendix F. Of course, the residuals shown there for Models 1 and 2 are not actually the residuals of the least squares fit. The latter were the basis for the fit in the logarithmic scale; the former were obtained by exponentiating the predicted logarithms and subtracting the result from the observed.

By varying individual parameters from the model while holding everything else constant, it is possible to visualize the individual effects of predictors. Figure 3-1 illustrates the effect of TDF feed fraction on emissions of CO (in ng/J total heat input), using nominal values of KILNT = 1000 °C, KILNGAS = 140 Nm³/hr, KILNFUEL = 9.1Nm³/hr, and KILNO2 = 7%, for each of Models 1 through 3. Notice that Models 1 and 2 are virtually indistinguishable from each other. Predicted COEMISFAC was insensitive to kiln temperatures and oxygen concentrations, and did not even exhibit a significant effect of TDF feed rate. Note that only the steady-state tests were used for all of the regression analysis.

The model would only predict an increase in CO emissions from a minimum of 10.3, to a maximum of 18.8 [ng/J total kiln fuel input] while increasing TDF from 0 % to 20 % of the kiln fuel input. Apparently, TDF combustion, when done in a steady-state mode, does not significantly increase CO emissions from those found during natural gas combustion.

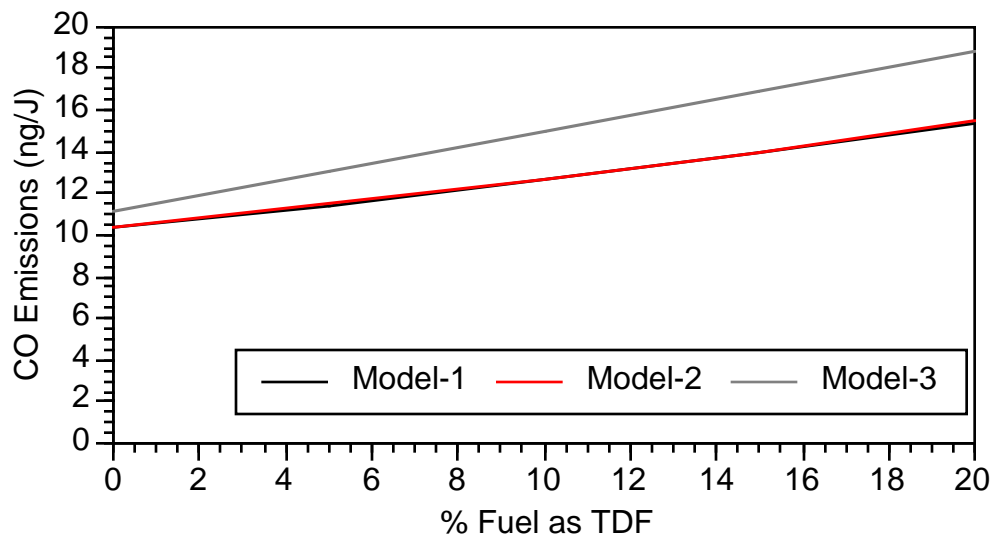


Figure 3-1. Model predictions: emissions of CO as a function of TDF feed rate; using KILNT = 1000 °C, KILNGAS=140 Nm³/hr, KILNFUEL=9.1Nm³/hr, and KILNO2 = 7%.

It was unusually difficult to pinpoint an optimal model for PAHEMISFAC. Of the three forms of PAH response attempted, linear, logarithmic, and reciprocal, ln(PAHEMISFAC) provided the greatest collection of acceptable alternative models. In fact, using SAS proc RSQUARE to examine all possible models, models were found containing 5, 6, 7, 8, and 9 predictors, all with $R^2 > 0.9$ and all of whose predictors were statistically significant at the 0.01 level ($p \leq 0.01$). Three predictor variables were shared in common between R^2 -optimal 5 and 9 term models, namely KILNGAS*KILNT, RKILNGAS, and FEED^2. Based on use of Mallows' C statistic, the data suggested the 9-term model to be most appropriate. Among the 5 - 9 term semi-log models, this is the preferred one, though the background "full" model used to reach this conclusion was based on only 4 error degrees of freedom, i.e., fitting a "FULL" model with 19 parameters to 23 data points. For the sake of comparison, we have included estimated coefficients and for both the R^2 -optimal 5-term (Model-1) and 9-term (Model-2) models for prediction of ln(PAHEMISFAC). The partial effect of each of the terms in the models is significant at the 0.01 level ($p \leq 0.01$).

A complete list of the residuals, i.e., [observed - fitted], for all 3 models can be found in Table F-3 in Appendix F. Of course, the residuals shown there for Models 1 and 2 are not actually the residuals of the least squares fit. The latter were the basis for the fit in the logarithmic scale; the former were obtained

by exponentiating the predicted logarithms and subtracting the result from the observed. Values shown in the following table are these differences multiplied by 10. As is evident in Table F-3, the shrinkage in absolute values of residuals is not universal in going from the best 5-term model to the best 9-term model, e.g., TB24 and TB27. Using linear PAHEMISFAC as the response variable, one 7-predictor model, labeled as Model-3, nearly satisfied all criteria for model selection. The exception was that $p \geq 0.0180$ for the partial effect of KILNGAS*KILNO2, whereas the p-values for testing the partial effects of all other predictors were universally ≤ 0.01 . However, it appears to be an excellent model, sharing four predictors in common with Model-2, having an acceptable $R^2 \geq 0.9410$, and having smaller absolute residuals, in general, than either Model-1 or Model-2. In addition, the data seemed to "home in" on the model, whereas with $\ln(\text{PAHEMISFAC})$ as the response, choice among 5 - 9 predictor models was not easy.

Figure 3-2 illustrates the effect of TDF feed rate on PAH emissions (as measured by the PAH analyzer), in ng/J total heat input, using nominal values of KILNT = 1000 °C, KILNGAS = 140 Nm³/hr, and KILNO2 = 7%, for each of Models 1 through 3. Notice how Models 2 and 3 are almost indistinguishable from one another. Increasing TDF feed from 0 to 20% increases the predicted PAH emissions from those of natural gas alone by approximately a factor of 5, from a minimum of 1.9E-4 to a maximum 1.1E-3 ng/J.

PAH emissions were fairly insensitive to temperature and oxygen over the range of conditions studied, although increasing TDF feed rates tended to increase PAH emissions for all oxygen levels. A useful objective for future TDF combustion studies would be to perform some basic research on TDF pyrolysis kinetics with special attention being given the transport phenomena in the vicinity of TDF particles. Overall, supplementing the fuel with TDF tends to increase PAH emissions, but not dramatically, provided steady-state operation is maintained.

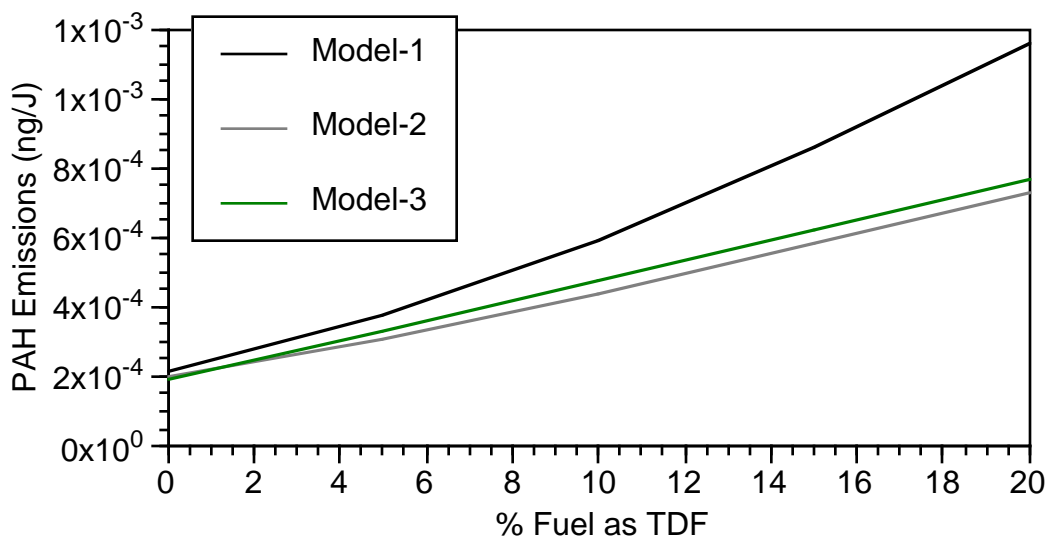


Figure 3-2. Model predictions: emissions of PAH as a function of TDF feed rate; using KILNT = 1000 °C, KILNGAS=140 Nm³/hr, and KILNO₂ = 7%.

3.2. Volatile Organic Samples

In general, the volatile organic compounds (VOCs) detected were fairly close to practical quantitation levels. A number of compounds identified in combustion samples were not present in the field blanks. However, several of the compounds found in combustion samples were also present in the field blanks at similar levels; primarily chloromethane, acetone, methylene chloride, and benzene. Benzene is a common PIC from combustion in general, and could be attributed to PICs from the natural gas flame found in the field blanks. However, benzene is also a breakdown product of Tenax, and acetone and methylene chloride are ubiquitous in laboratory environments. In addition, some samples contained trichlorofluoromethane, which is a chlorofluorocarbon commonly used in air conditioners. Appendix B contains all of the volatile organic data. Table 3-7 summarizes the results from the volatile organic samples, by averaging the emission values from all compounds that were present in concentrations greater than the quantitation level on at least one VOST tube. On compounds where one or more VOST tubes had concentrations below the quantitation level, then the quantitation level was used for averaging. The results from the trichlorofluoromethane, acetone and methylene chloride are considered suspect, and are not reported in Table 3-7. Standard deviations are reported in parenthesis.

To evaluate the differences between conditions with and without TDF, average reported concentrations from Table 3-7 were divided by the reported concentration for the 0 % TDF case (the natural gas blank), and any values that resulted in a ratio less than 2.0 for all runs were discarded. The results from this calculation are illustrated in Figure 3-3. Although emissions of most compounds during TDF combustion were not significantly different from those resulting from natural gas

combustion, there were several significant differences. Emissions of chloromethane, benzene, and styrene were consistently higher while firing TDF.

Tires contain trace amounts of chlorine, which can apparently combine with other PICs present to form chloromethane. The absence of other higher molecular weight chlorinated organics suggests that the TDF chlorine was not initially associated with the organic tire matrix, but was possibly present in the inorganic parts of the tire. The TDF analysis did not attempt to determine whether the TDF chlorine was organic or inorganic, however, there may be chlorinated rubber in tires.

Benzene emissions were much higher while the RKIS was operating in a non-steady mode. This appears to indicate that TDF combustion can produce elevated levels of aromatic PICs when not combusted in a steady-state mode. Styrene emissions were approximately 3 times higher than those found during natural gas combustion, regardless of the amount of TDF being burned. Emissions of carbon disulfide and toluene were elevated during the test when TDF was batch fed into the RKIS. These PICs are indicative of fuel-rich combustion. Xylene levels were also elevated during the batch test.

Interestingly, some PICs were reduced below levels found from natural gas combustion during unsteady TDF combustion, most notably, 2-methyl propene. Levels of 2-methyl propene increased with the addition of TDF during steady-state operation, but were reduced during transient operation. It is possible that during non-steady operation, local fuel-rich zones developed which promoted aromatic ring growth from substituted alkenes.

Table 3-7. Summary of VOC concentrations (ng/L).

compound	TB5 0 % TDF (blank)	TB1 7 % TDF (steady- state)	TB3 17 % TDF (steady- state)	TB8 19 % TDF (ramp)	TB9 15 % TDF (batch)
1,1,1, trichloroethane	0.55 (0.04)	0.88 (0.33)	1.00 (0.34)	0.52 (0.01)	0.47 (0.05)
2-methyl propene	2.36 (0.92)	5.40 (3.40)	4.38 (1.08)	1.70 (0.65)	0.50 (0.03)
2-methyl-2-propanol	0.52 (0.01)	0.51 (0.03)	4.10 (6.20)	0.52 (0.01)	0.50 (0.03)
benzene	1.65 (0.24)	2.93 (0.91)	2.83 (0.80)	17.00 (16.11)	47.31 (53.91)
bromomethane	0.49 (0.06)	0.51 (0.03)	0.58 (0.11)	2.82 (1.68)	0.83 (0.64)
carbon disulfide	0.52 (0.01)	0.81 (0.62)	0.52 (0.00)	0.52 (0.01)	2.04 (2.68)
chlorobenzene	0.52 (0.01)	0.51 (0.03)	0.52 (0.00)	0.52 (0.01)	0.48 (0.04)
chloromethane	0.59 (0.11)	1.68 (2.17)	8.81 (12.36)	55.03 (28.38)	11.17 (6.67)
ethyl benzene	0.52 (0.01)	0.51 (0.03)	0.61 (0.06)	0.52 (0.01)	1.07 (0.25)
heptane	0.52 (0.01)	0.67 (0.31)	0.56 (0.17)	0.52 (0.01)	0.50 (0.03)
hexane	0.49 (0.06)	0.58 (0.16)	0.55 (0.06)	0.52 (0.01)	0.51 (0.01)
iodomethane	0.52 (0.01)	0.51 (0.03)	0.52 (0.00)	0.54 (0.05)	0.50 (0.03)
m,p-xylene	1.52 (0.17)	0.98 (0.40)	2.40 (0.29)	0.61 (0.12)	3.85 (1.11)
nonane	0.68 (0.15)	1.72 (0.47)	0.96 (0.40)	0.52 (0.01)	0.59 (0.15)
o-xylene	0.45 (0.06)	0.51 (0.03)	0.72 (0.07)	0.52 (0.01)	1.13 (0.33)
styrene	0.65 (0.32)	1.85 (0.37)	1.62 (1.54)	1.62 (1.05)	1.69 (0.36)
toluene	0.97 (0.35)	1.18 (0.65)	1.05 (0.24)	0.80 (0.18)	2.78 (0.91)

In order to compare these quantities to other sources in the real world, it is appropriate to express the emissions of these various VOC compounds as emission factors in terms of ng/J heat input. There are two ways to perform the conversion; with or without taking into account the contribution from the natural gas. Table 3-8 lists the estimated emissions of the same compounds in terms of ng/J, by including both the natural gas and TDF contributions. Table 3-9 lists the estimated emissions with only taking into account the TDF contribution, by dividing the results from Table 3-8 by the fraction of TDF fed (i.e., the blank concentrations were not subtracted out prior to dividing by the TDF fraction). It should be noted that emissions from a unit that burns 100 % TDF are not likely to be a linear extrapolation from the 10-20 % levels being co-fired here. There is very little literature on VOC emission factors from conventional combustion devices burning coal or oil, but there are data for formaldehyde emission factors in the literature.²⁷ Average emission factors for formaldehyde emissions from oil-fired combustion sources average around $1.74\text{E-}1$ ng/J, and for coal, $7.32\text{E-}2$ ng/J, which are on the same order of magnitude, if not slightly higher, than those found during these tests. This finding suggests that VOC emissions from a properly run facility burning TDF are not significantly different from a properly operated facility burning conventional fossil fuels.

As an illustration of the differences between emissions from burning TDF in a controlled manner, as opposed to uncontrolled combustion as is found in a tire fire, using data reported from a study examining emissions from the simulated open burning of scrap tires,⁹ estimated benzene emissions were

approximately 280 ng/J, which is approximately 5 orders of magnitude higher than those found in this study.

Table 3-8. Estimated emissions of VOCs (ng/J), based on TDF + natural gas.

compound	TB5	TB1	TB3	TB8	TB9
	0 % TDF (blank)	7 % TDF (steady-state)	17 % TDF (steady-state)	19 % TDF (ramp)	15 % TDF (batch)
1,1,1, trichloroethane	2.24E-04	3.75E-04	4.41E-04	2.24E-04	2.17E-04
2-methyl propene	9.60E-04	2.30E-03	1.94E-03	7.37E-04	2.33E-04
2-methyl-2-propanol	2.13E-04	2.15E-04	1.81E-03	2.24E-04	2.33E-04
benzene	6.71E-04	1.25E-03	1.25E-03	7.36E-03	2.19E-02
bromomethane	2.00E-04	2.15E-04	2.58E-04	1.22E-03	3.82E-04
carbon disulfide	2.13E-04	3.43E-04	2.30E-04	2.24E-04	9.43E-04
chlorobenzene	2.13E-04	2.15E-04	2.30E-04	2.24E-04	2.20E-04
chloromethane	2.40E-04	7.15E-04	3.90E-03	2.38E-02	5.16E-03
ethyl benzene	2.13E-04	2.15E-04	2.70E-04	2.24E-04	4.96E-04
heptane	2.13E-04	2.83E-04	2.48E-04	2.24E-04	2.33E-04
hexane	2.01E-04	2.45E-04	2.45E-04	2.24E-04	2.36E-04
iodomethane	2.13E-04	2.15E-04	2.30E-04	2.35E-04	2.33E-04
m,p-xylene	6.21E-04	4.17E-04	1.06E-03	2.64E-04	1.78E-03
nonane	2.77E-04	7.29E-04	4.25E-04	2.24E-04	2.71E-04
o-xylene	1.85E-04	2.15E-04	3.18E-04	2.24E-04	5.24E-04
styrene	2.63E-04	7.85E-04	7.16E-04	7.03E-04	7.80E-04
toluene	3.97E-04	5.02E-04	4.64E-04	3.48E-04	1.29E-03

Table 3-9. Estimated emissions of VOCs (ng/J), based on TDF only.

compound	TB1	TB3	TB8	TB9
	7 % TDF (steady-state)	17 % TDF (steady-state)	19 % TDF (ramp)	15 % TDF (batch)
1,1,1, trichloroethane	5.36E-03	2.59E-03	1.18E-03	1.45E-03
2-methyl propene	3.28E-02	1.14E-02	3.88E-03	1.55E-03
2-methyl-2-propanol	3.07E-03	1.07E-02	1.18E-03	1.55E-03
benzene	1.78E-02	7.35E-03	3.87E-02	1.46E-01
bromomethane	3.07E-03	1.52E-03	6.42E-03	2.55E-03
carbon disulfide	4.90E-03	1.35E-03	1.18E-03	6.29E-03
chlorobenzene	3.07E-03	1.35E-03	1.18E-03	1.47E-03
chloromethane	1.02E-02	2.29E-02	1.25E-01	3.44E-02
ethyl benzene	3.07E-03	1.59E-03	1.18E-03	3.31E-03
heptane	4.04E-03	1.46E-03	1.18E-03	1.55E-03
hexane	3.51E-03	1.44E-03	1.18E-03	1.57E-03
iodomethane	3.07E-03	1.35E-03	1.24E-03	1.55E-03
m,p-xylene	5.95E-03	6.23E-03	1.39E-03	1.19E-02
nonane	1.04E-02	2.50E-03	1.18E-03	1.81E-03
o-xylene	3.07E-03	1.87E-03	1.18E-03	3.49E-03
styrene	1.12E-02	4.21E-03	3.70E-03	5.20E-03
toluene	7.17E-03	2.73E-03	1.83E-03	8.58E-03

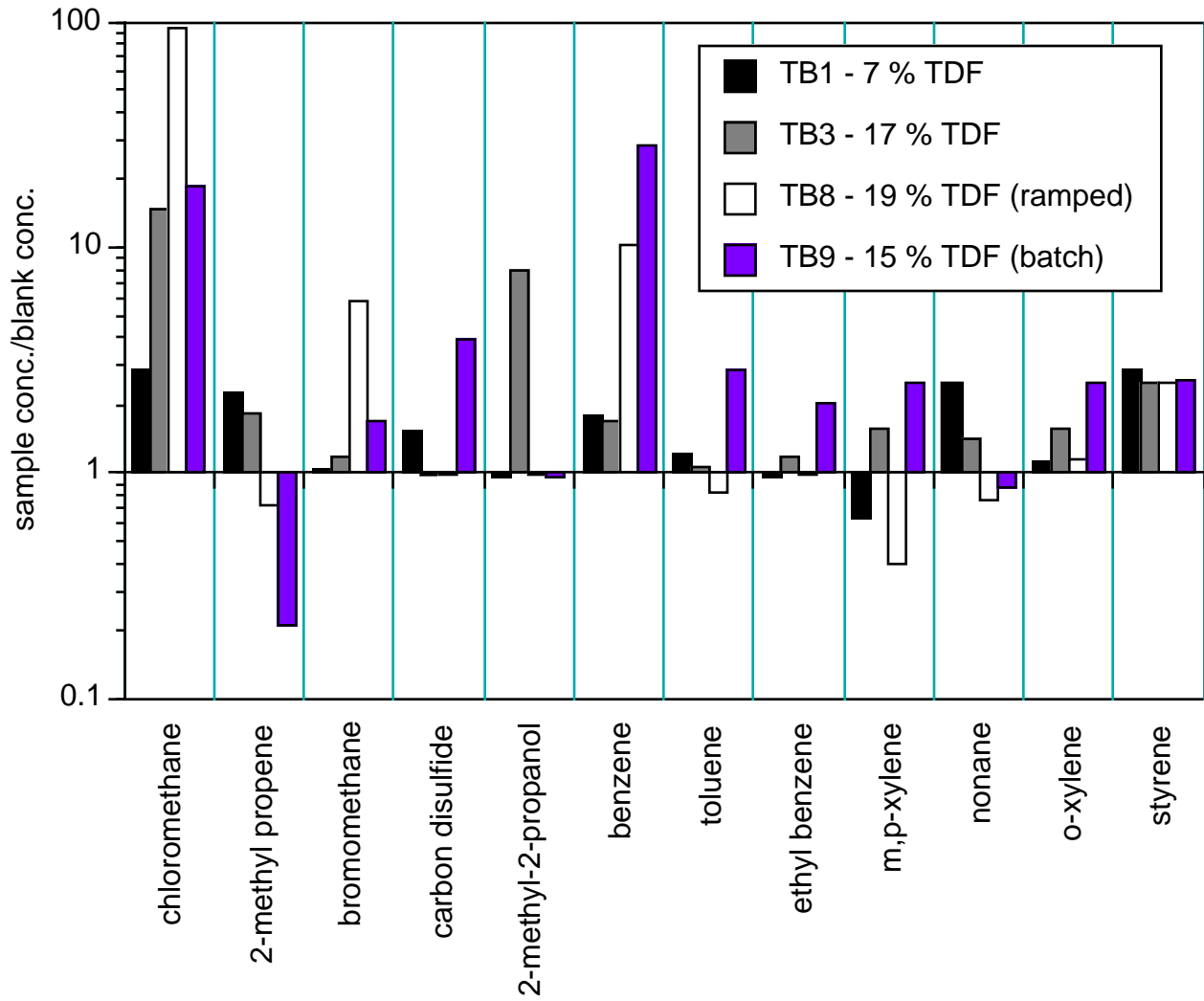


Figure 3-3. Comparison of VOC emissions between natural gas and TDF combustion.

3.3. Semi-Volatile Organic Samples

3.3.1. MM5 Sampling Trains

The complete SVOC analysis results are found in Appendix C. The results from the semi-volatile organic compound (SVOC) analyses do not seem to indicate the presence of SVOCs in detectable concentrations. Trace quantities of phenol were identified in several samples. Several phthalates were present in two samples. A wide variety of phthalates are used as plasticizers and are common laboratory contaminants. The presence of these phthalates as contaminants seems more plausible than their being PICs. However, no phthalates were found in the field blank.

As with the volatile organic analyses, surrogate standards were added to the SVOC samples to assess method performance. For several samples, achieved recovery values were less than target values, which indicates possible target loss. Recovery performance data for each sample are included in Appendix C.

For two samples (TB4 - 17 % TDF steady-state and TB9 - 15 % TDF batch), the "less than" concentrations reported are a factor of ten greater than the remaining results reported. These samples were taken to provide bioassay analyses, and as such, required TCO and GRAV analyses. These samples therefore had a larger final extract volume. It is for this reason that no surrogate recovery performance data are given as well, since the surrogate standards might have generated a false positive response on the bioassays. The bioassay results will be reported in a different document.

3.3.2. Continuous PAH Analyzer

As illustrated in Table 3-2, the PAH analyzer gave readings on all steady-state tests ranging up to 3289 ng/Nm³, which converts into 3.3 µg/Nm³. This concentration is below the method detection level for individual PAH compounds in the SVOC analysis. Considering that other past experiences with the PAH analyzer gave good agreement with conventional SVOC analyses,^{28,29} it can be surmised that the results reported from the PAH analyzer compare favorably with the PAH concentrations that were actually present in the stack. At any rate, the PAH analyzer did not give a false positive signal, and, as shown in Figure 3-4, tracked O₂ and CO₂ quite well during the ramping test (TB8), in spite of the fact that CO emissions did not significantly change. This observation suggests that the PAH analyzer is quite sensitive to minor system disturbances, and may be useful for process control purposes.

Overall, it appears that when combusted in a well-operated facility, emissions of SVOCs from TDF combustion are not significantly different than from natural gas.

3.4. PCDD/PCDF Samples

Complete PCDD and PCDF sampling and analytical results are found in Appendix D. PCDD/PCDF samples (Method 23) were collected during only 2 test conditions: TB7 - 0 % TDF (combustion blank) and TB6 - 17 % TDF steady-state. The results of the PCDD/PCDF analyses indicate that PCDDs and PCDFs were not detected during these tests. The results from the TB6 - 17 % TDF test reveals that hexachlorodibenzofuran was present at a concentration essentially equal to the method detection limit. Similarly, the results from the combustion background test (TB7 - 0 % TDF) revealed that tetrachlorodibenzodioxin was present at a concentration also essentially equal to the method detection limit. The method blank did not detect either of these target analytes.

Since detectable quantities of chloromethane were found in several of the VOC samples, and since chlorine is present in small quantities in the TDF material, it may be possible that higher levels of PCDD and PCDF might be found from a full-scale combustion system, since it has been shown that a significant amount of formation of PCDD/PCDF occurs in the particulate control devices at temperatures around 300 °C, although moderate amounts of PCDD/PCDF formation can occur on in-flight particles.³⁰ In these tests, there was no particulate control device installed, so concentrations reported here only would represent those found in the transition duct between the combustor and any particulate control device. At any rate, though, it would be expected that PCDD/PCDF emissions would be low.

3.5. Metals Samples

Appendix E contains all of the metals emissions data. Metal aerosol samples (MMT) were collected during only 2 test conditions: TB7 - 0 % TDF (combustion blank) and TB6 - 17 % TDF steady-state. The intent was to analyze the front and back halves of the sampling train separately to gain insight into the distribution of metal aerosols. Unfortunately, the back half sample from the TB6 - 17 % TDF feed test was damaged during shipment and was not capable of being analyzed. The liquid from this damaged sample may have also contaminated the front half sample of the TB7 - 0 % TDF feed test (blank), since relatively high concentrations of lead and zinc were found in this fraction. The presence of these 2 metals may also be attributable to the fact that the combustion blank was collected after a number of TDF tests had been performed, and a hysteresis effect might have occurred. This possibility is supported by the presence of zinc and lead in the back half fraction of the blank sample, which would not be affected by the damaged sample. Table 3-10 lists the concentrations of metals and Table 3-11 lists the estimated emissions for the two tests where sampling occurred. If we repeat the treatment given

the VOC emissions by comparing the metal emissions from these TDF combustion tests to emission factors from coal and oil in the literature, we can examine the emissions of these metal species with a point of reference that is more well understood. Note that the linear extrapolation based on TDF feed fraction is more likely to be valid for metals than for organics.

Table 3-10. Stack concentration ($\mu\text{g}/\text{m}^3$) of metals from TDF combustion.

metal	TB7 0% TDF (blank)	TB6 17 % TDF (steady-state)
antimony	0.18	2.11
arsenic	1.12	37.16
beryllium	nd	0.05
cadmium	0.41	1.06
chromium	0.65	3.88
lead	8.05	65.96
manganese	2.82	5.79
nickel	0.71	3.51
selenium	0.83	4.50
zinc	286.94	35465

nd - none detected.

Table 3-11. Estimated metals emissions (ng/J) from TDF combustion.

metal	TB7 0% TDF (blank)		TB6 17 % TDF (steady-state)	
	TDF+natural gas	TDF only	TDF+natural gas	TDF only
antimony	7.72E-5	n/a	9.05E-4	5.32E-3
arsenic	4.80E-4	n/a	1.59E-2	9.35E-2
beryllium	nd	n/a	2.14E-5	1.26E-4
cadmium	1.76E-4	n/a	4.54E-4	2.67E-3
chromium	2.78E-4	n/a	1.66E-3	9.76E-3
lead	3.45E-3	n/a	2.83E-2	1.66E-1
manganese	1.21E-3	n/a	2.48E-3	1.46E-2
nickel	3.0E-4	n/a	1.50E-3	8.82E-3
selenium	3.56E-4	n/a	1.93E-3	1.14E-2
zinc	1.23E-1	n/a	15.21	89.47

n/a - not applicable

The literature²⁷ reports the values found in Table 3-12 for emission factors from coal and oil for various metals. To derive the average emission factors reported here, uncontrolled values for oil from reference 27 were averaged for both distillate and residual oil, and values for coal from uncontrolled dry bottom utility boilers burning bituminous coal. By comparing Tables 3-11 and 3-12, it is apparent that, with the exception of zinc, uncontrolled metal emissions from TDF combustion are similar in magnitude to those for coal and oil. TDF combustion gives high Zn emissions due to the fact that there are high

levels of Zn in tires, coupled with the fact that Zn is a volatile metal that tends to be emitted in the flyash as opposed to remaining in the bottom ash residue.

Table 3-12. Average emission factors for coal- and oil-fired boilers (ng/J).

metal	oil	coal
antimony	n/a	n/a
arsenic	5.00E-03	2.95E-01
beryllium	1.44E-03	3.48E-02
cadmium	5.64E-03	1.91E-02
chromium	1.49E-02	6.07E-01
lead	7.95E-03	1.36E-01
manganese	8.61E-03	1.28E+00
nickel	3.08E-01	5.00E-01
selenium	n/a	n/a
zinc	n/a	n/a

n/a - not available
Source: Reference 27

3.6 Particulate Data

Particulate matter (PM) measurements were made from the MM5 and MultiMetals trains. PM measurements are not routinely made from MM5 trains as the typical Method 5 acetone front half rinse and evaporation procedures are not compatible with the sample treatments leading to organic analyses. However, the MM5 sampling was the only particulate collection method common to all tests. The particulate data reported here are based on the total mass of particulate collected on the filter as well as the cyclone located upstream of the filter. All front half rinses were submitted for organic analysis. The complete PM data are found in Appendix F.

The MultiMetals train is suitable for determining total particulate loading as the front half acetone rinse and evaporation step is optional. Particulate values are also reported for the two tests where metals samples were collected.

Table 3-13 lists the results for the PM measurements. The PM measurements listed represent uncontrolled emissions, such as those found prior to any installed PM control device. As expected, the PM emissions during TDF combustion are higher than those from natural gas combustion. Interestingly, the PM results from run TB9 (the batch feed run) were significantly higher than for the other runs. The MM5 filter on this run was blacker than on the other runs.

3.7. XRD/XRF Results

After each run, there was a significant amount of ash residue deposited on the TDF feeding mechanism. Samples from runs TB3 and TB6 were collected and analyzed for elemental composition with X-ray fluorescence spectrometry. For this analysis, the samples were mixed with an organic binder and pressed into pellets. The samples were first scanned for qualitative characterization. For better accuracy, it is necessary to set up a quantitative scheme based on the matrix composition. Since the composition was similar to fly ash, that scheme was applied. Element concentrations determined by this method are reported here to two significant figures. Note that some elements identified from the XRF analysis (e.g., zirconium, aluminum, and silicon) may have originated in the RKIS refractory insulation, and not from the TDF. Results also confirm the high Zn emissions found in the MMT samples. The concentrations for the balance of the elements detected, in the qualitative scan, are reported to one significant figure. Table 3-14 lists the results from the XRF analysis.

Table 3-13. Particulate data.

Run	% Total Fuel as TDF	Particulate Loading (mg/Nm³)
TB2	16.95	43.67 ⁺⁺
TB3	17.14	137.24 ⁺⁺
TB4	15.50	95.28 ⁺⁺
TB5	0.00	17.37 ⁺⁺
TB8+	19.18	132.95 ⁺⁺
TB9+	14.97	285.46 ⁺⁺
TB6	17.30	101.01
TB7	0.00	4.14

+ non-continuous feed tests

++ based on filter weights from MM5 or Method 23 samples

Table 3-14. TDF fly ash composition (wt %) as determined by X-ray fluorescence.

element	TB3	TB6
aluminum	2.8	1.9
calcium	3.1	2.9
chromium	0.002	0.01
cobalt	0.005	0.01
copper	0.002	0.0001
iron	0.86	0.83
lead	0.001	0.0009
magnesium	0.86	0.95
nickel	0.007	0.003
phosphorus	0.001	0.0001
potassium	0.58	0.58
silicon	32	32
sodium	0.68	1.2
strontium	0.002	0.01
sulfur	0.0004	0.0003
titanium	0.15	0.084
zinc	2.4	5.2
zirconium	0.01	0.01

X-ray diffraction spectrometry (XRD) was also carried out on the two samples to determine the phases of the major elements. XRD is usually capable of detecting phases down to several percent. The phases identified in the two samples are listed in the following table. Because of the many factors which influence XRD reflections, it is mainly of value for qualitative rather than quantitative analysis. In certain cases, where matrices are similar and sample preparation is controlled, it may be used for quantitative analyses. For this analysis, the phases are listed in estimated order of decreasing concentration. The XRD spectra for TB3 and TB6 can be found in Appendix F. Table 3-15 lists the results from the XRD analysis.

Table 3-15. TDF fly ash composition as determined by X-ray diffraction.

name	formula	JCPDS No.	present in TB3	present in TB6
			sample	sample
crystalite	SiO ₂	39-1425	X	X
quartz	SiO ₂	33-1161	X	X
willemite	Zn ₂ SiO ₄	37-1496	X	X
anhydrite	CaSO ₄	37-1496	X	X
mullite	Al ₆ Si ₂ O ₁₃	15-776	X	-

3.8. Effect of Transient Operation

Selected traces from the CEMs during the TB8 test, where the kiln combustion air was ramped up and down, are shown in Figures 3-4 through 3-8. Notice how the O₂ and CO₂ traces (Figures 3-4 and 3-5) oscillate in a sinusoidal manner to mirror the changes in the combustion air. The fact that the response time (≈ 2 s) for the PAH analyzer was considerably faster than the response time for the CO analyzer (≈ 30 s), coupled with the fact that the PAH analyzer (see Figure 3-6) was considerably more sensitive to minor system disturbances during periods of "good" combustion than the CO analyzer (see Figure 3-7 and 3-8), suggests that the PAH analyzer might prove to be an effective monitor for process control purposes. These data seem to suggest that pyrolysis at the surface of the TDF particles is one of the rate controlling steps for TDF combustion. Although the TDF was not burning in suspension phase, the low feed rates that were used during these tests resulted in a fairly dispersed bed of burning TDF particles scattered around the recessed chamber of the kiln. As such, it may be a valid assumption that individual TDF particles were burning with little or no influence from nearby TDF particles. The transport of the pyrolysis products away from the TDF particles, coupled with some boundary layer resistance, appear to significantly affect the emission of PICs from TDF combustion. By ramping the combustion air up and down, it appears that the boundary layer surrounding the TDF particles is subjected to some transient disturbances, possibly de-stabilizing the flame front that is in place at the outside of the particle's boundary layer. This phenomenon might result in increased PIC emissions.

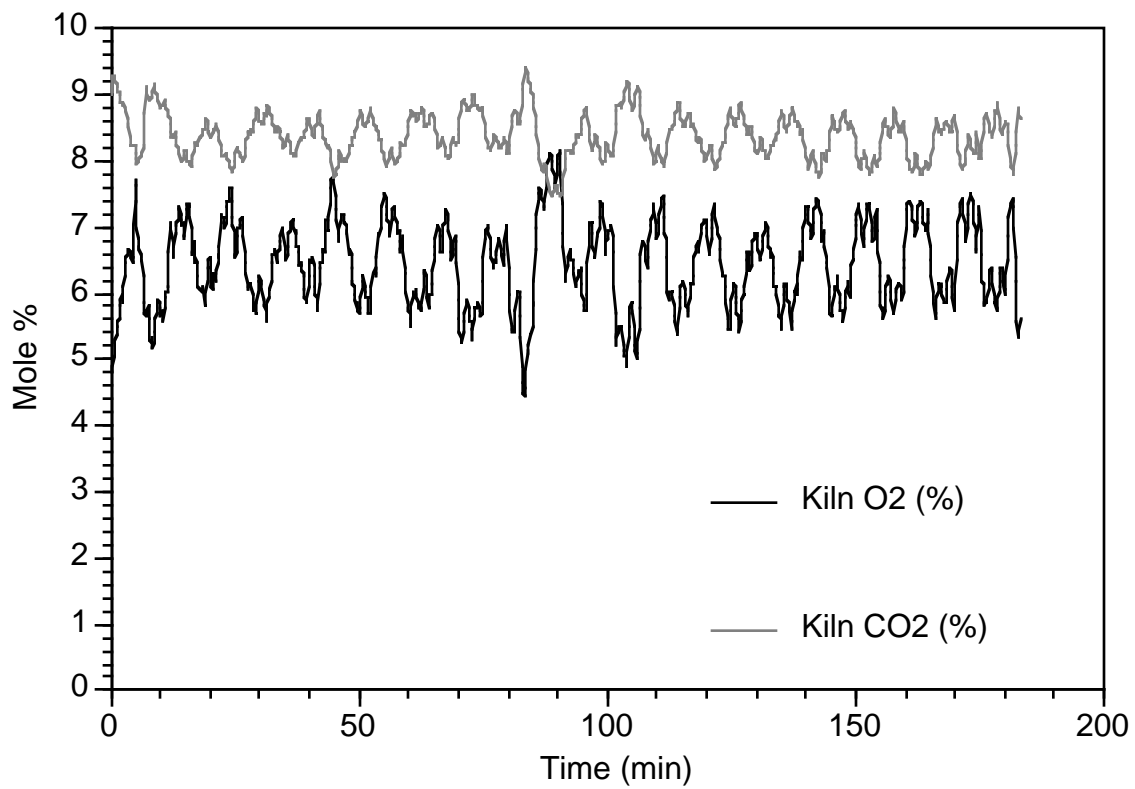


Figure 3-4. Kiln O₂ and CO₂ traces during run TB8.

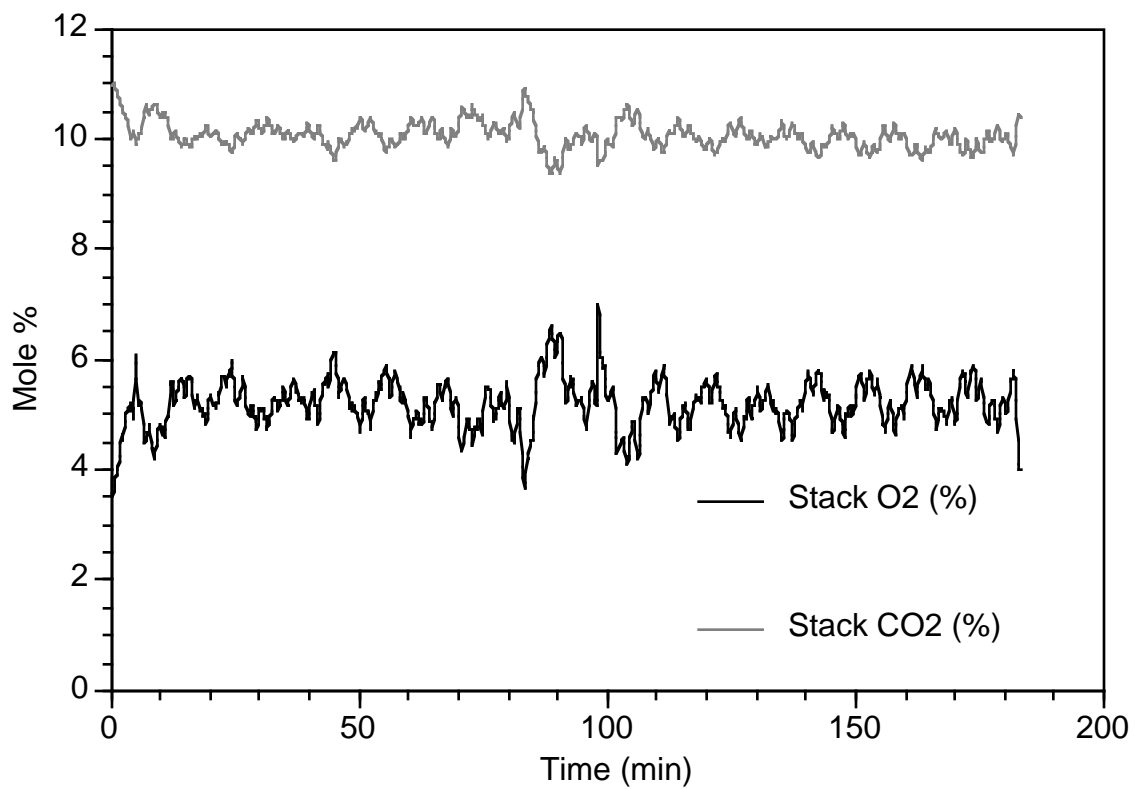


Figure 3-5. Stack O₂ and CO₂ traces during run TB8.

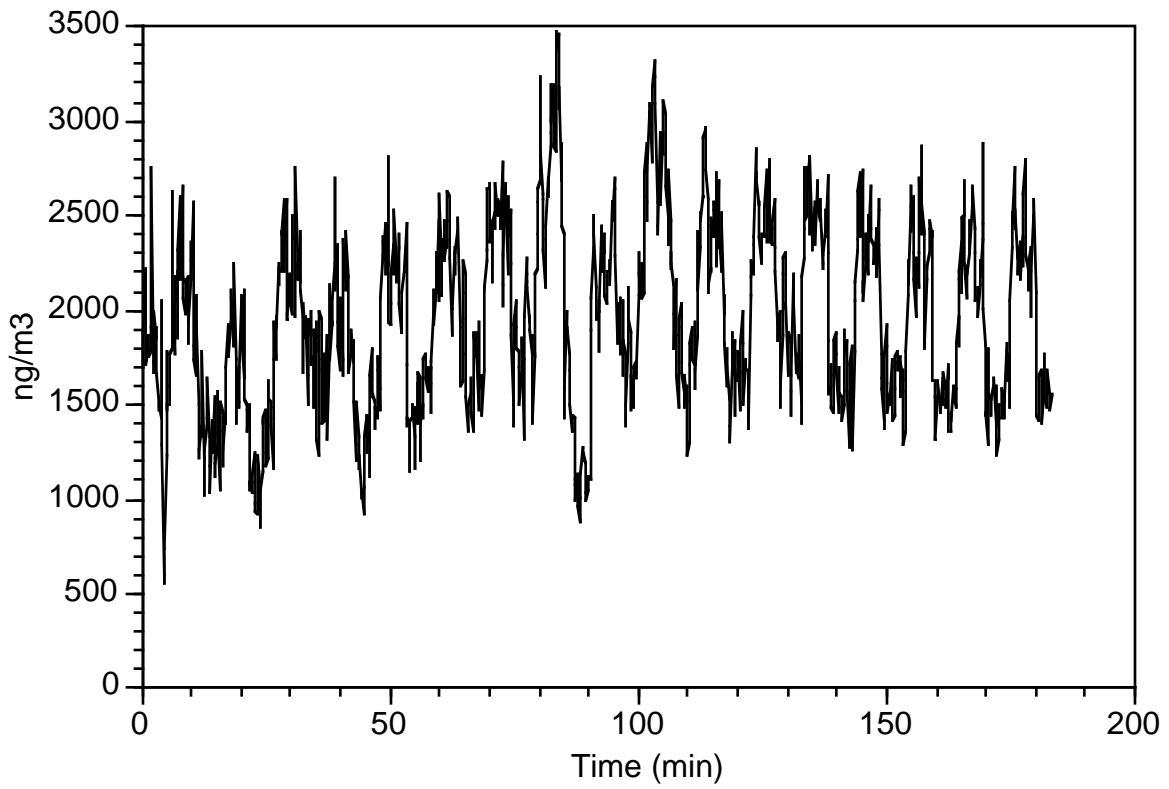


Figure 3-6. PAH analyzer trace during run TB8.

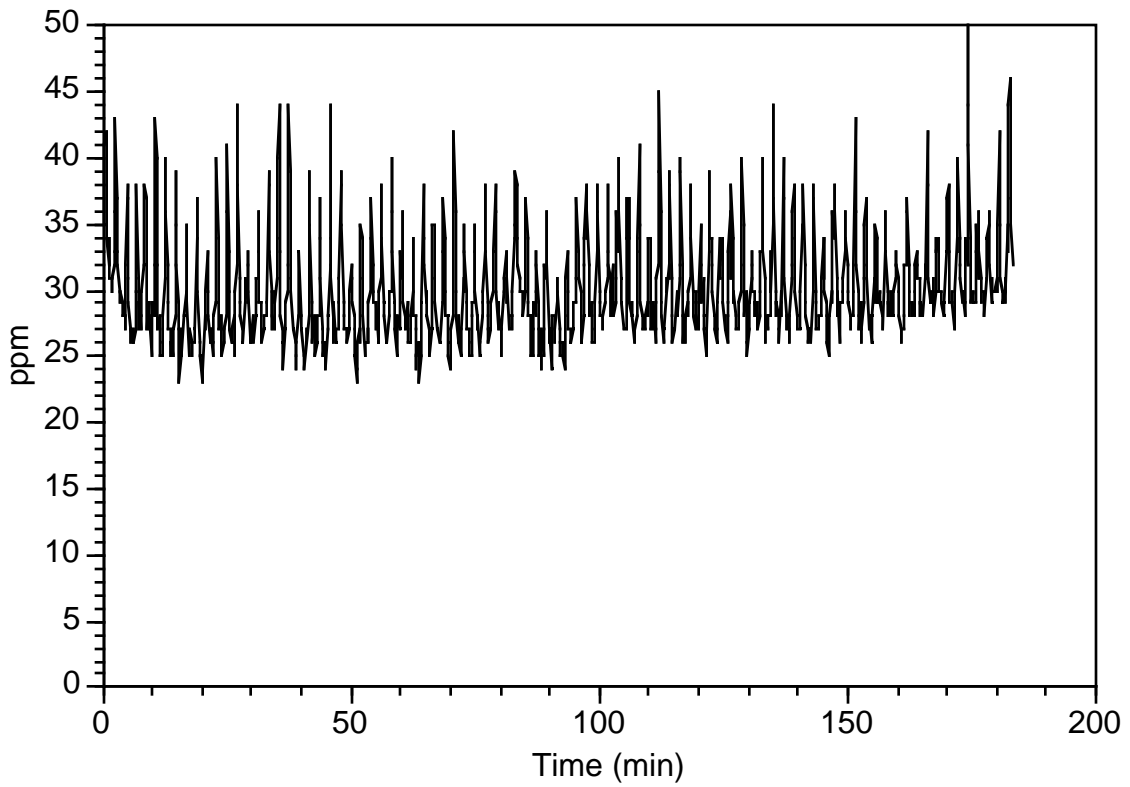


Figure 3-7. Kiln CO traces during run TB8.

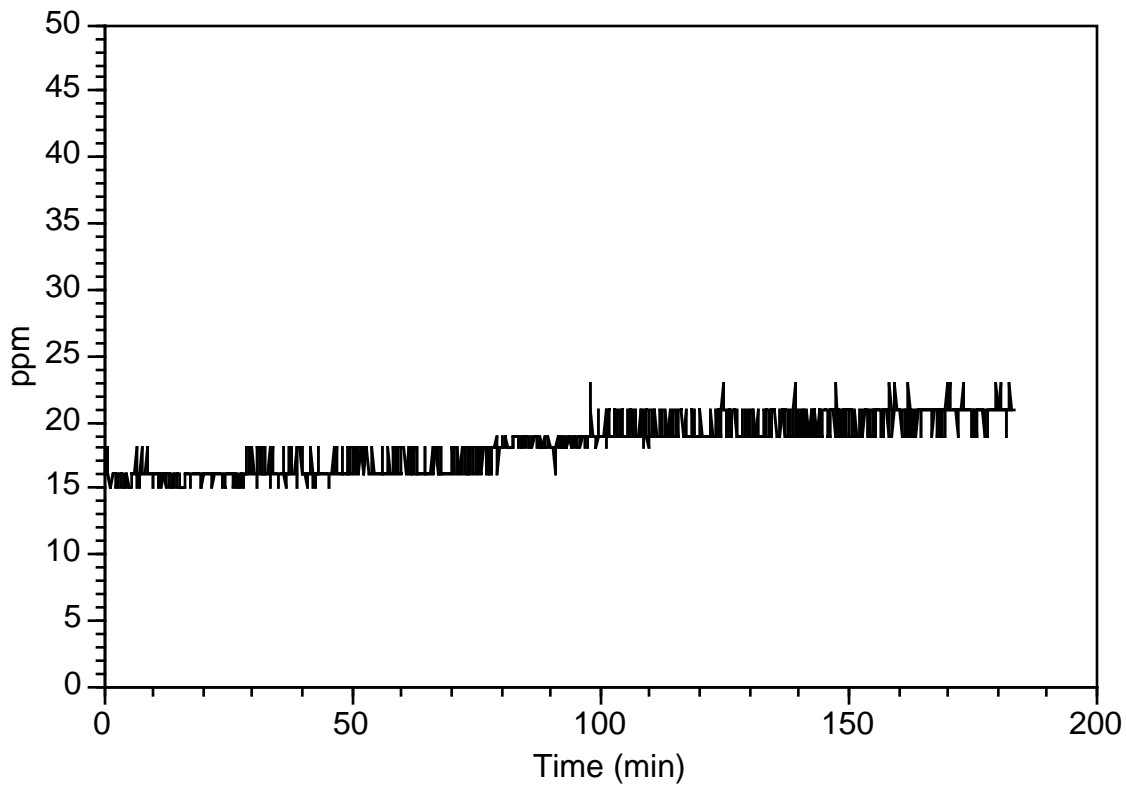


Figure 3-8. Stack CO traces during run TB8.

Selected traces from the CEMs during the TB9 test, where batches of TDF were fed at discreet intervals, are shown in Figures 3-9 through 3-13. The batch tests resulted in very high transient emissions followed by periods of essentially background emission levels. Notice how the kiln O₂ (see Figure 3-9), initially at approximately 10 %, plummets to approximately 1 % during the batch introduction of TDF. Even the post-SCC stack O₂ (see Figure 3-10) is reduced to just over 2 % during the transients. The PAH analyzer (see Figure 3-11) measured a high (214,000 ng/m³) average concentration on the TB9 batch test, which was not found on the corresponding MM5 train samples for SVOCs. However, since the transient events resulting from batch feeding of TDF were very short relative to the total sampling time, the required isokinetic sampling protocols may have resulted in an insufficient sample being pulled into the MM5 train. These results are qualitatively similar to results seen from earlier batch feed tests on this same facility while burning polyethylene pipe,¹⁴ where non-isokinetic sampling procedures and larger sampling volumes were required to produce detectable quantities of individual compounds. Note also how the PAH analyzer (Figure 3-11) tracks the CO traces (Figures 3-12 and 3-13) very well. As mentioned earlier, the CO analyzer is an acceptable diagnostic for "poor" combustion conditions, but cannot effectively differentiate between different levels of "good" combustion.

These data suggest that burning TDF in batches, which roughly approximates feeding of whole tires, has the potential to form significant transient emissions. This phenomena could be exacerbated in a system that exhibits significant vertical gas-phase stratification, or operates at low excess air levels, such as cement kilns. The size of the facility, however, will certainly impact the intensity of transient emissions resulting from batch charging of tires or TDF, since for an extremely large facility, a constant stream of whole tires may roughly approximate steady-state operation. Even so, the potential for generation of large transients should not be ignored.

These two transient experiments highlight the limitations of using CO as a surrogate indicator of combustor performance. While CO is high during periods of "poor" combustion, as is evidenced during the batch feed tests, CO does not give a good indication of de-tuned combustor performance during periods of relatively "good" combustion. In other words, the CO analyzer is effective as a diagnostic of "poor" combustion, but cannot differentiate between "good" and "great" combustion.

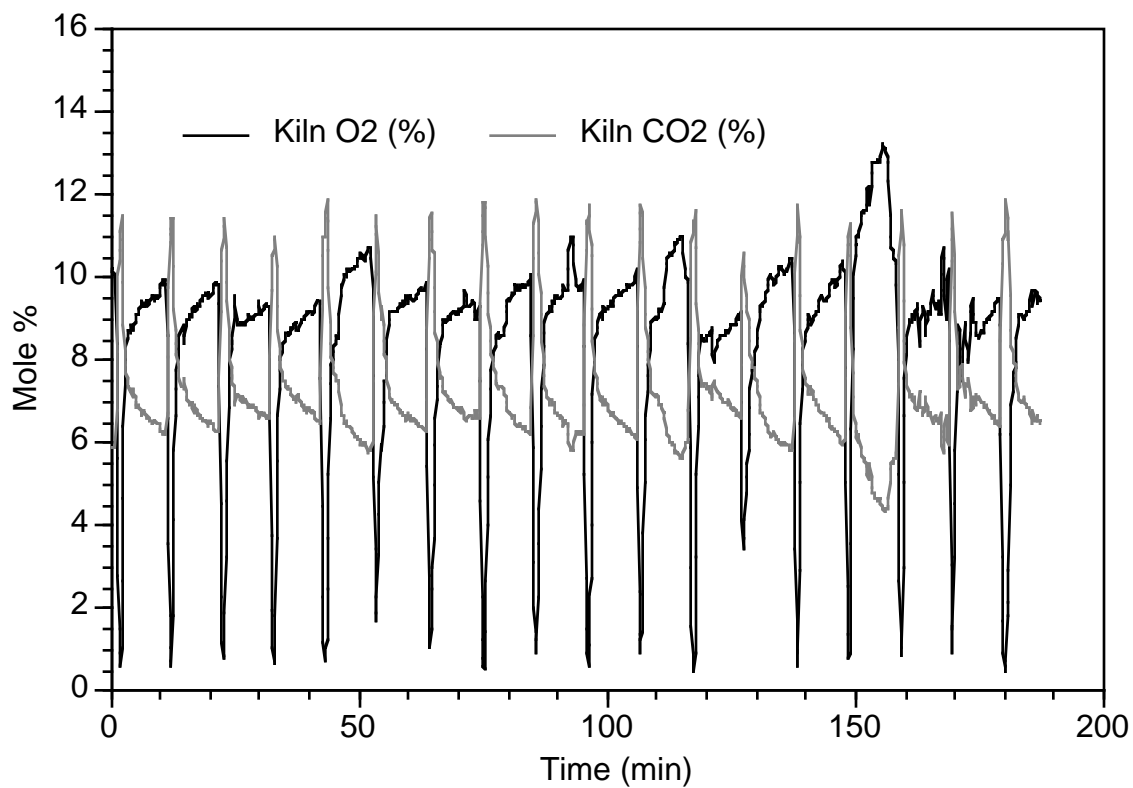


Figure 3-9. Kiln O₂ and CO₂ traces during run TB9.

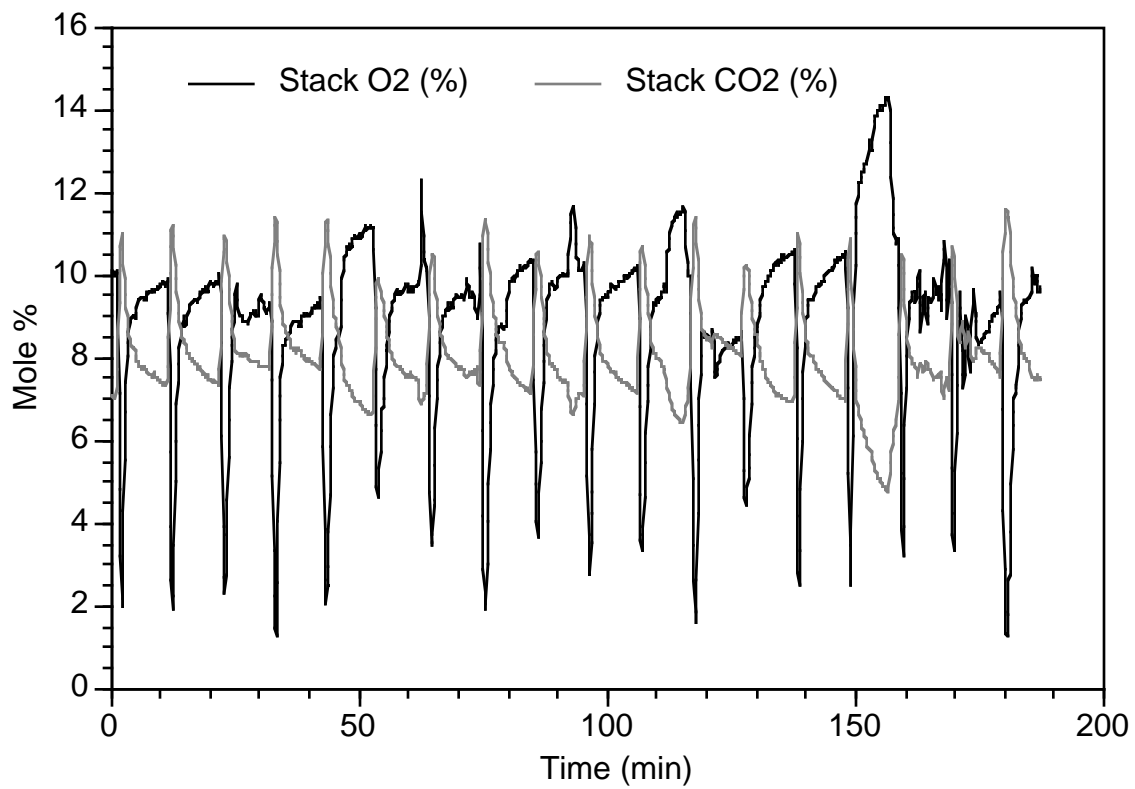


Figure 3-10. Stack O₂ and CO₂ traces during run TB9.

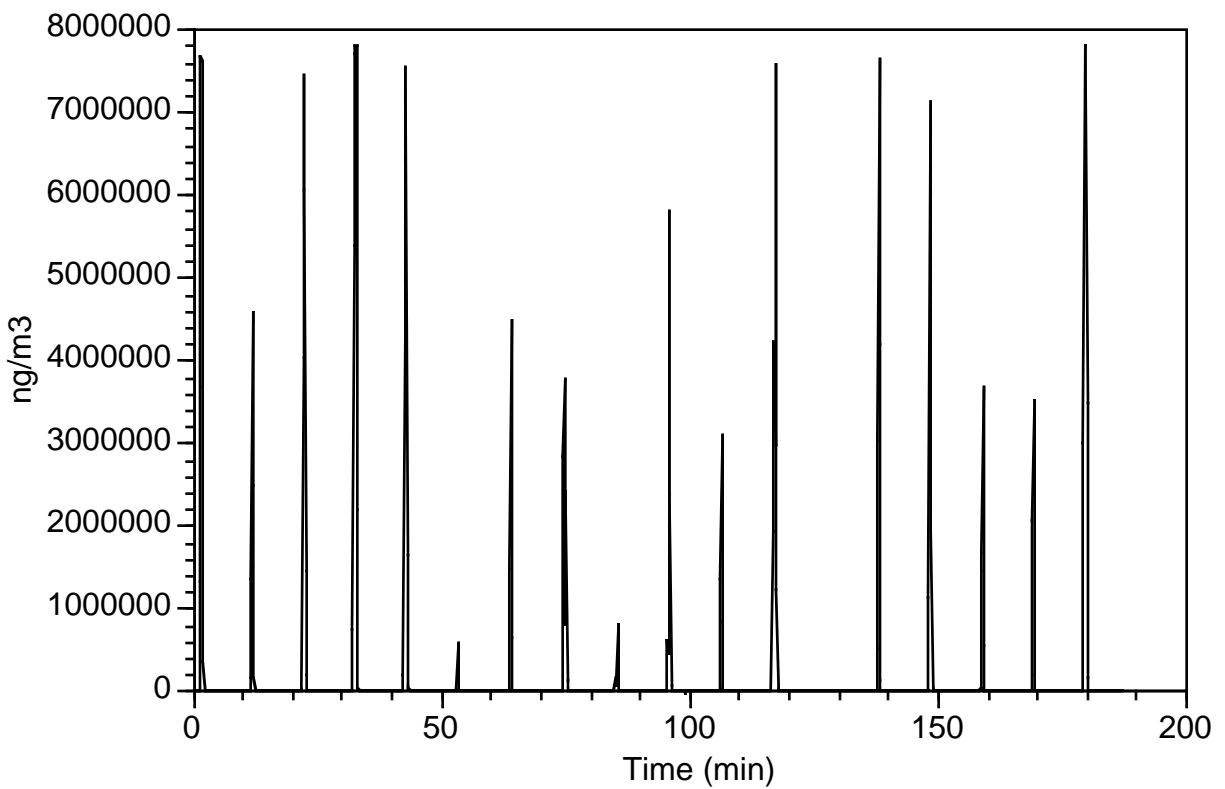


Figure 3-11. PAH analyzer trace during run TB9.

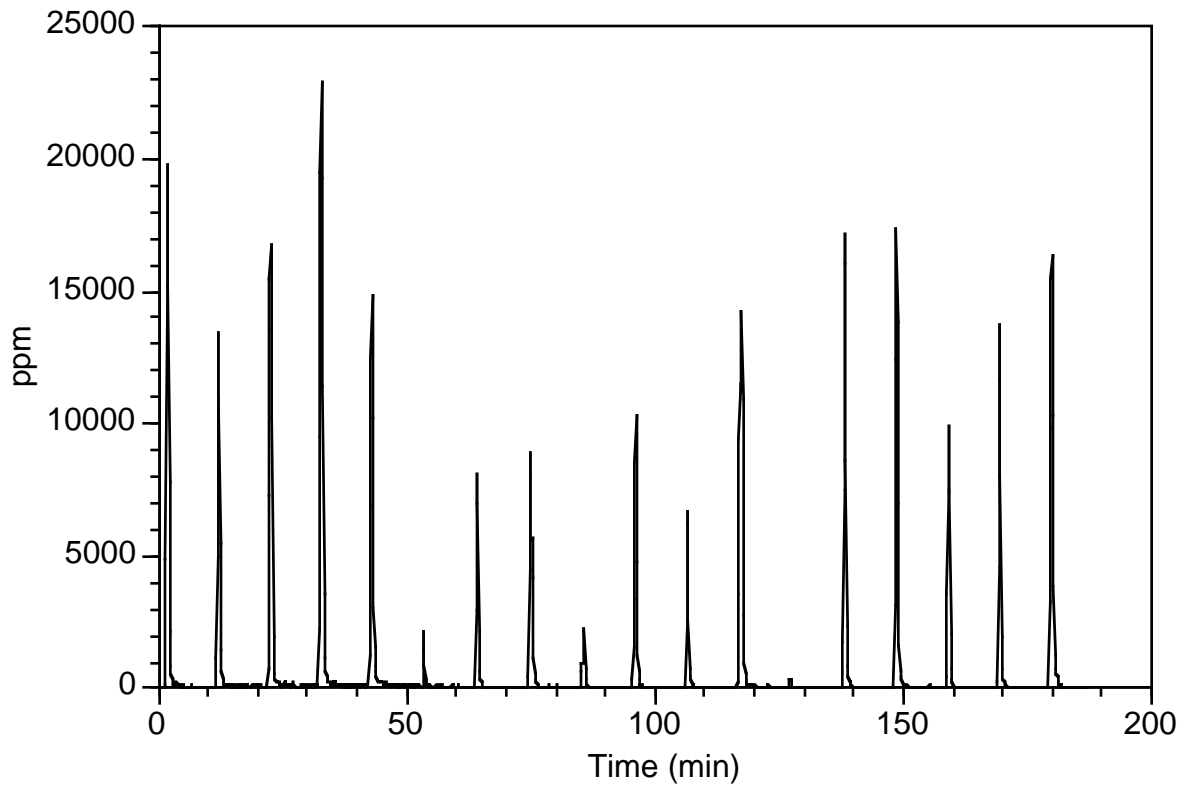


Figure 3-12. Kiln CO traces during run TB9.

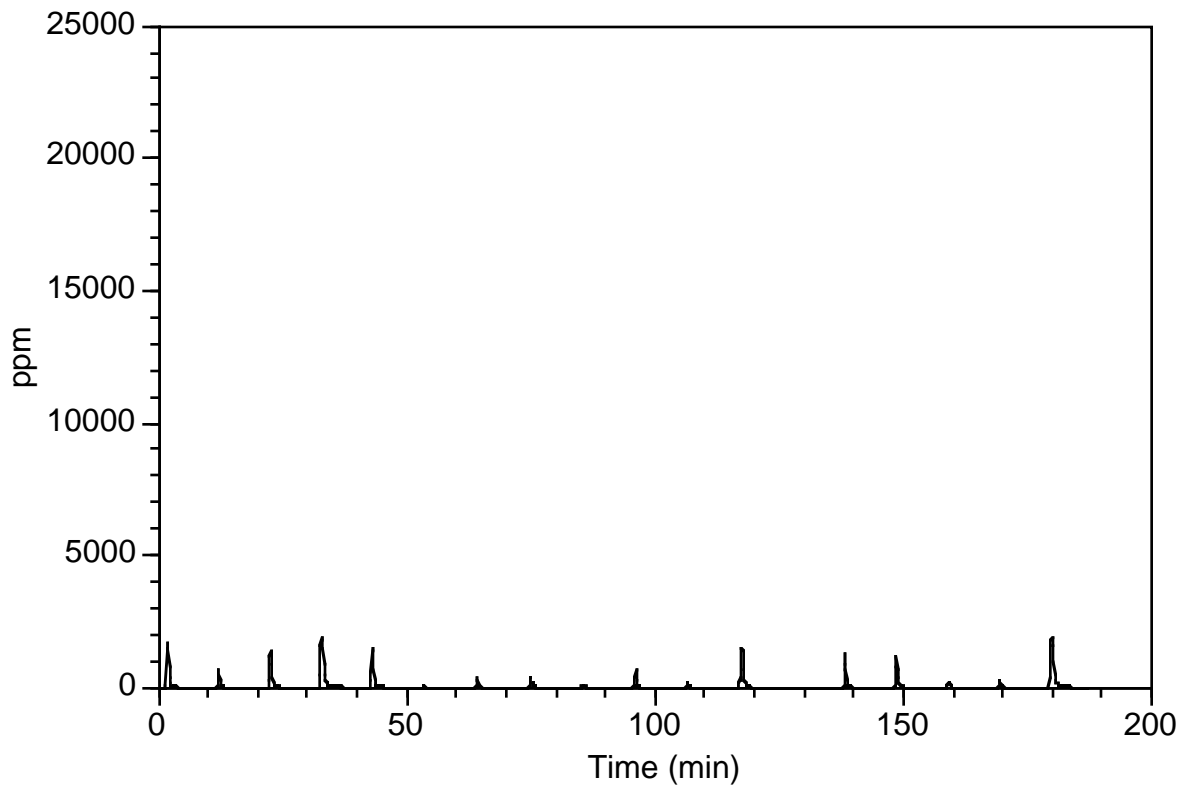


Figure 3-13. Stack CO traces during run TB9.

4. CONCLUSIONS

A series of experiments were performed on a bench-scale rotary kiln incinerator simulator (RKIS) facility to examine HAPs from combustion of TDF. Both steady-state and transient testing was performed so that an evaluation of continuous vs. incremental TDF feeding could be achieved. Samples were analyzed continuously by CEM for O₂, CO, CO₂, NO, THC_s, SO₂, and PAH_s. VOST, MM5, Method 23, and MMT samples were collected to analyze for VOC_s, SVOC_s, PCDD/PCDF, and metal aerosols, respectively. X-ray diffraction and X-ray fluorescence techniques were used to identify species in the fly ash. A regression analysis was completed on the CEM data to examine pollutant emission trends.

Several VOC_s were identified, particularly chloromethane, benzene, and styrene. The concentrations of those VOC_s was affected by the amount and mode of TDF feeding. Emissions of benzene, in particular, are particularly sensitive to transient upsets of the combustion process. Comparison of calculated emission factors to those found in the literature for conventional fossil fuel combustion indicate that VOC emissions from TDF combustion are comparable to those from coal and oil combustion.

No significant amounts of SVOC_s were identified. The PAH analyzer indicated PAH concentrations on the same order as the detection level of the SVOC analytical methods, with the exception of the test where TDF was batch fed to the RKIS facility. The PAH analyzer indicated considerably higher transient concentrations of PAH_s during batch feeding, however, these elevated PAH levels were not detected with the MM5 samples. It is possible that the short duration of the transients, coupled with the mandatory isokinetic sampling protocols, prevented sufficient amounts of pollutants from being sampled.

Emission levels of PCDD and PCDF were found to be similar in magnitude to the combustion blank which consisted of a natural gas flame. Those congeners of PCDD and PCDF identified in all samples were on the same order of magnitude as the method detection level.

Elevated levels of arsenic, lead, and zinc were found in the stack gas. Zinc was present in significant concentrations. Analysis of the fly ash residue indicate that the majority of the particulate matter was SiO₂, Al₆Si₂O₁₃, and Zn₂SiO₄. Comparison of calculated emission factors from TDF combustion to those found in the literature for conventional fossil fuel combustion suggests that, with the exception of zinc, the magnitudes of metal emissions are similar to coal and oil, although the distributions are

significantly different, especially with respect to emissions of mercury and selenium, which are significantly higher from coal combustion.

The PAH analyzer tracked transient kiln operation during periods of "good" combustion more effectively than the CO analyzer, and with a faster response. It may be significantly more effective than CO for process control applications due to its sensitivity. Regression analysis of PAH analyzer measurements indicated that an approximately five-fold increase (over natural gas emissions) in PAH emissions occurs while increasing the TDF fuel input fraction from 0 to 20%.

Regression analysis of CO emissions from the steady-state tests did not find a significant correlation with kiln operating conditions. A slight increase in CO emissions with increasing TDF feed rate was found.

The results suggest that burning TDF in batches, such as during the feeding of whole tires, has the potential to form significant transient emissions. This phenomenon could be exacerbated in a system that exhibits significant vertical gas-phase stratification, or operates at low excess air levels, such as cement kilns. The size of the facility, however, will certainly impact the intensity of transient emissions resulting from batch charging of tires or TDF, since for an extremely large facility, a constant stream of whole tires may roughly approximate steady-state operation. Even so, the potential for generation of large transients should not be ignored, especially in smaller facilities.

Data gaps still exist, since this limited study was performed on a small combustor, under controlled conditions. The following issues might be addressed in future research.

- The effect of TDF particle size and feeding mode on HAP emissions should be investigated more fully. This study was done using a single TDF particle size, and included only limited testing on different feeding modes.
- Emissions of HAPs from combustion of wire-in TDF should be investigated. It would be logical to assume that emissions of metals from combustion of wire-in TDF may be significantly different than from TDF that has had the wire removed. Combustion temperature would likely affect metals emissions significantly, since the partitioning of metals between the bottom ash residue and the fly ash would change.
- Characteristics of other TDF-generated residues, such as bottom ash, should be investigated, especially in regards to leachability of metals, and slag composition and quality.

- Emissions of HAPs from co-firing of TDF with other solid fuels, such as coal, biomass-derived fuels, municipal solid waste, or refuse-derived fuel should be investigated.
- The characteristics of TDF-generated flyash should be investigated more fully, including the particle size distributions and speciation of the metals, especially as a function of halogens or sulfur which might be present due to co-firing of other fuels.
- Some basic research, on a very small scale, should be performed, to examine the chemistry of TDF pyrolysis and combustion.
- Tests on other types of facilities (such as a vertically-fired unit) should be performed. Studies examining TDF combustion in suspension vs. bed-burning phases should be performed.

Overall, it appears that, with the exception of zinc, potential emissions from TDF combustion are not significantly different from emissions from combustion of conventional fossil fuels, when burned in a well-designed and well-operated combustion device. If unacceptable particulate loading occurs due to zinc emissions, then the emissions would have to be controlled by an appropriate particulate control device.

5. REFERENCES

- ¹ Sladek, T.A. Workshop on Disposal Techniques with Energy Recovery for Scrapped Vehicle Tires, City and County of Denver, The Energy Task Force of the Urban Consortium for Technology Initiatives, U.S. Department of Energy, Denver, CO, 101 pp, February 1987.
- ² Kearney, A.T. Scrap Tire Use/Disposal Study, Prepared for the Scrap Tire Management Council, Washington, DC, September 1990.
- ³ Clark, C., K. Meardon, and D. Russell Burning Tires for Fuel and Tire Pyrolysis: Air Implications, EPA-450/3-91-024 (NTIS PB92-145358), December 1991.
- ⁴ Pirnie, M. Air Emissions Associated with the Combustion of Scrap Tires for Energy Recovery, Prepared for the Ohio Air Quality Development Authority, Columbus, OH, May 1991.
- ⁵ Section 1038, H.R. 2950 Intermodal Surface Transportation Efficiency Act of 1991. First Session of the 102nd Congress. Enacted December 18, 1991.
- ⁶ Haverfield, L.E. and B.L. Hoffman "Used Tires as a Means of Dispersal of Aedes aegypti in Texas." *Mosq. News*, 26:433-5, 1966.
- ⁷ Miller, R.D. "Managing Scrap Tires: What Role Should State and Local Government Play?" In Workshop on Disposal Techniques with Energy Recovery for Scrapped Vehicle Tires, City and County of Denver, The Energy Task Force of the Urban Consortium for Technology Initiatives, U.S. Department of Energy, Denver, CO, February 1987.
- ⁸ Ryan, J.V. Characterization of Emissions from the Simulated Open Burning of Scrap Tires, EPA-600/2-89-054 (NTIS PB90-126004), October 1989.
- ⁹ Lemieux, P.M. and J.V. Ryan, (1993) "Characterization of Air Pollutants Emitted from a Simulated Scrap Tire Fire," *J. AWMA*, 43: 1106-1115.
- ¹⁰ Lemieux, P.M. and D.M. DeMarini, "Mutagenicity of Emissions from the Simulated Open Burning of Scrap Rubber Tires," EPA-600/R-92-127 (NTIS PB92-217009), July 1992.
- ¹¹ DeMarini, D.M., P.M. Lemieux, J.V. Ryan, L.R. Brooks, and R.W. Williams, (1994) "Mutagenicity and Chemical Analysis of Emissions from the Open Burning of Scrap Rubber Tires," *Environ. Sci. Technol.*, Vol. 28, No. 1, 136-141.

¹² Jones, R.M., J.M. Kennedy, Jr., and N.L. Heberer, "Supplementary Firing of Tire-Derived Fuel (TDF) in a Combination Fuel Boiler," TAPPI Journal, May 1990.

¹³ Clean Air Act Amendments of 1990, Public Law 101-549, November 15, 1990.

¹⁴ Linak, W.P., J.D. Kilgroe, J.A. McSorley, J.O.L. Wendt, and J.E. Dunn, (1987), On the Occurrence of Transient Puffs in a Rotary Kiln Incinerator Simulator I. Prototype Solid Plastic Wastes, *J. Air Poll. Cont. Assoc.*, **37**, 54.

¹⁵ Linak, W.P., J.A. McSorley, J.O.L. Wendt, and J.E. Dunn, (1987), On the Occurrence of Transient Puffs in a Rotary Kiln Incinerator Simulator II. Contained Liquid Wastes on Sorbent, *J. Air Poll. Cont. Assoc.*, **37**, 934.

¹⁶ Cundy, V.A., T.W. Lester, A.M. Sterling, A.N. Montestruc, J.S. Morse, C.B. Leger, and S. Acharya, (1989), "Rotary Kiln Incineration III. An Indepth Study - Kiln Exit/Afterburner/Stack Train and Kiln Exit Pattern Factor Measurements During Liquid CCl₄ Processing," *J. Air Poll. Cont. Assoc.*, **39**, 944-952.

¹⁷ Method 0030, "Volatile Organic Sampling Train," in Test Methods for Evaluating Solid Waste, Volume II: Field Manual Physical/Chemical Methods, EPA-SW-846 (NTIS PB 88-239223), 3rd ed., U.S. Environmental Protection Agency, Washington, DC, September 1986.

¹⁸ Method 5040, "Protocol for Analysis of Sorbent Cartridges from Volatile Organic Sampling Train," in Test Methods for Evaluating Solid Waste, Volume IB: Laboratory Manual Physical/Chemical Methods, EPA-SW-846 (NTIS PB 88-239223), 3rd ed., U.S. Environmental Protection Agency, Washington, DC, September 1986.

¹⁹ Method 8240, "Gas Chromatography/Mass Spectrometry for Volatile Organics," in Test Methods for Evaluating Solid Waste, Volume IB: Laboratory Manual Physical/Chemical Methods, EPA-SW-846 (NTIS PB 88-239223), 3rd ed., U.S. Environmental Protection Agency, Washington, DC, September 1986.

²⁰ Method 0010, "Modified Method 5 Sampling Train," in Test Methods for Evaluating Solid Waste, Volume II: Field Manual Physical/Chemical Methods, EPA-SW-846 (NTIS PB 88-239223), 3rd ed., U.S. Environmental Protection Agency, Washington, DC, September 1986.

²¹ Method 8270, "Gas Chromatography/Mass Spectrometry for Semivolatile Organics: Capillary Column Technique," in Test Methods for Evaluating Solid Waste, Volume IB: Laboratory Manual Physical/Chemical Methods, EPA-SW-846 (NTIS PB 88-239223), 3rd ed., U.S. Environmental Protection Agency, Washington, DC, September 1986.

²² Gang, S., "Methodology for the Determination of Metals Emissions in Exhaust Gases from Hazardous Waste

Incineration and Similar Combustion Processes," in Methods Manual for Compliance with the BIF Regulations, Burning Hazardous Waste in Boilers and Industrial Furnaces, EPA/530-SW-91-010 (NTIS PB91-120006) U.S. Environmental Protection Agency, Washington, D.C. December 1990.

²³ Method 23 in Title 40 Code of Federal Regulations Part 60, Appendix A, U.S. Government Printing Office, Washington, D.C. 1991.

²⁴ Method 8280 in Test Methods for Evaluating Solid Waste, Volume 1B: Laboratory Manual Physical/Chemical Methods, EPA-SW-846 (NTIS PB 88-239223), 3rd ed., U.S. Environmental Protection Agency, Washington, D.C., September 1986.

²⁵ Lemieux, P.M., "Computer-Aided Data Acquisition for Combustion Experiments," *Scientific Computing and Automation*, Vol 9, No. 5, April 1993.

²⁶ Hicks, C.R., (1973), *Fundamental Concepts in the Design of Experiments*, 2nd ed., Holt, Rinehart and Winston Inc., New York, NY.

²⁷ Brooks, G., "Estimating Air Toxics Emissions from Coal and Oil Combustion Sources," EPA-450/2-89-001 (NTIS PB89-194229), April 1989.

²⁸ Lutes, C.C. and J.V. Ryan, "Characterization of Air Emissions from the Simulated Open Combustion of Fiberglass Materials," EPA-600/R-93-239 (NTIS PB94-136231), December 1993.

²⁹ Chikhliwala, E.D., J.W. Podlenske, E. Pfeiffer, and W. Seifert, "The Design, Implementation, and Use of a Real-time PAH Analyzer for Combustion Products," Paper presented at the 9th World Clean Air Congress & Exhibition, Montreal, Canada, August 1992.

³⁰ Gullett, B.K., P.M. Lemieux, and J.E. Dunn, (1994) "Role of Combustion and Sorbent Parameters in Prevention of Polychlorinated Dibenzo-p-dioxin and Polychlorinated Dibenzofuran Formation During Waste Combustion," *Environ. Sci. Technol.*, Vol. 28, No. 1, 107-118.

APPENDIX A. QA/QC EVALUATION REPORT

This project was performed under the Level III Quality Assurance Project Plan entitled "Combustion of Scrap Tires in a Rotary Kiln", and assigned QTRAK #86016/III. All critical measurements met the data quality objectives satisfactorily. Certain non-critical measurements, such as NO and SO₂ did not meet data quality objectives. However, the QA goals of the project were met.

A.1. Volatile Organic Samples

In general, the volatile organic compounds detected were fairly close to practical quantitation levels. A number of the compounds identified in combustion samples were not present in the field blanks. However, several of the compounds found in combustion samples were also present in the field blanks at similar levels; primarily chloromethane, acetone, and methylene chloride. Acetone and methylene chloride are ubiquitous in laboratory environments. Each VOST tube was individually QC checked so as to ensure that species measured would indeed originate in the stack. No tube contained more than 10 ng of any compound. The VOST tube QC checks did not indicate inherent contamination at these levels. Therefore, the results from these compounds should be considered somewhat suspect. All analytical method performance criteria were met during analysis of these samples. Appendix B contains all of the VOC data, including surrogate compound recovery.

A.2. Semi-Volatile Organic Samples

The results from the semi-volatile organic compound (SVOC) analyses do not seem to indicate the presence of SVOCs in significant concentrations. Trace quantities of phenol were identified in several samples. Several phthalates were present in two samples. A wide variety of phthalates are used as plasticizers and are common laboratory contaminants. The presence of these phthalates as contaminants seems more plausible than their being PICs. However, no phthalates were found in the field blank.

As with the volatile organic analyses, surrogate standards were added to the SVOC samples to assess method performance. For several samples, achieved recovery values were less than target values. It is possible that targets were lost on these samples. Recovery performance data for each sample, as well as isokinetic sampling information, are included in Appendix C.

For two samples (20% TDF steady-state and 20% TDF batch), the "less than" concentrations reported are a factor of ten greater than the remaining results reported. These samples were taken to provide bioassay analyses, and as such, required TCO and GRAV analyses. These samples therefore had a larger final extract volume. It is for this reason that no surrogate recovery performance data are given as well, since the surrogate standards might have generated a false positive response on the bioassays.

A.3. PCDD/PCDF Samples

PCDD/PCDF samples (Method 23) were collected during only 2 test conditions: 0 % TDF (combustion blank) and 20% TDF steady-state. The results of the PCDD/PCDF analyses indicate that PCDDs and PCDFs were not detected during these tests. The results from the 20% TDF test reveals that hexachlorodibenzofuran was present at a concentration essentially equal to the method detection limit. Similarly, the results from the combustion background test (no TDF) revealed that tetrachlorodibenzodioxin was present at a concentration also essentially equal to the method detection limit. The method blank did not detect either of these target analytes. Appendix D contains all of the data regarding the

PCDD/PCDF analyses, including isokinetic sampling information and surrogate standard recovery information.

A.4. Metals Samples

Metals samples (Method 29) were also only collected during only 2 test conditions: 0 % TDF (combustion blank) and 20% TDF steady-state. The intent was to analyze the front and back halves of the sampling train separately to gain insight into the distribution of metal aerosols. Unfortunately, the back half sample from the 20% TDF feed test was damaged during shipment and was not capable of being analyzed. The liquid from this damaged sample may have also contaminated the front half sample of the 0% TDF feed test (blank), since relatively high concentrations of lead and zinc were found in this fraction. The presence of these 2 metals may also be attributable to the fact that the combustion blank was collected after a number of TDF tests had been performed, and a hysteresis effect might have occurred. This possibility is supported by the presence of zinc and lead in the back half fraction of the blank sample, which was not affected by the damaged sample. Appendix E contains all of the data regarding the metals analyses, including surrogate compound recovery and isokinetic sampling information.

A.5. QCER for CEM Data

A 3-point calibration was performed on each CEM daily. The data collected for each test were validated by post-test zero and span checks. The results of post-test CEM zero and span checks are presented in Table A-1. The overall accuracy, precision, and completeness data quality indicator (DQI) levels achieved along with respective DQI goals for each CEM measurement are presented in Table A-2. As Tables A-1 and A-2 indicate, difficulties were encountered with the NO and SO₂ measurements. Excessive drift was encountered during many of the tests performed. Fortunately, these were not critical measurements, and the lack of data for these measurements does not compromise the quality of this study.

A.6. General QA Information

Appendix F contains other analytical data, including a summary of all extractive sampling, dates of individual runs, and the XRD spectra. Isokinetic variation is based on a single point location sampling relative to the highest velocity traverse point established during the pre-test velocity traverse. The highest velocity location was selected to maximize collected sample volumes. With the exception of the test performed on 5/11/93, all test samples were collected within acceptance of method isokinetic variation limits. The pretest velocity traverses, along with determined moisture levels, were also used to derive volumetric stack flows.

Table A-2. Data quality indicator results for CEM measurements.

Meas.	Accuracy *		Precision @		Completeness	
	Goal	Achiev. #	Goal	Achiev.	Goal	Achiev.
O ₂	< 3	0.4	< 10	1.4	> 90	100
CO ₂	< 3	0.5	< 10	0.7	> 90	100
CO	< 3	0.4	< 10	1.2	> 90	100
NO	< 3	5.2	< 10	8.5	> 90	11
THC	< 3	0.3	< 10	5.1	> 90	100
SO ₂	< 3	3.2	< 10	17.7	> 90	44

* Accuracy expressed as percent bias from full scale of measurement range.

Based on overall absolute value average of zero and span checks.

@ Expressed as percent relative standard deviation

APPENDIX B. VOLATILE ORGANIC SAMPLING DATA
(NOT AVAILABLE IN DIGITAL FORMAT)

APPENDIX C. SEMI-VOLATILE ORGANIC SAMPLING DATA
(NOT AVAILABLE IN DIGITAL FORMAT)

APPENDIX D. PCDD/PCDF DATA
(NOT AVAILABLE IN DIGITAL FORMAT)

APPENDIX E. METALS DATA
(NOT AVAILABLE IN DIGITAL FORMAT)

APPENDIX F. OTHER DATA

Table F-1. Kiln tire burn runs.

Date	Run
4/29/93	TB1
5/11/93	TB2
5/13/93	TB3
5/17/93	TB4
5/18/93	TB5
5/19/93	TB6
5/20/93	TB7
5/21/93	TB8
5/25/93	TB9
5/26/93	TB10
5/26/93	TB11
5/26/93	TB12
5/26/93	TB13
5/26/93	TB14
5/26/93	TB15
5/26/93	TB16
5/26/93	TB17
5/26/93	TB18
5/26/93	TB19
5/26/93	TB20
5/26/93	TB21
5/26/93	TB22
5/27/93	TB23
5/27/93	TB24
5/27/93	TB25
5/27/93	TB26
5/27/93	TB27
5/27/93	TB28
5/27/93	TB29
5/27/93	TB30

Table F-2. Kiln Tire Burns Sampling Summary.

Table F-3. Kiln Tire Burn Particulate Summary

Test Run	Date	Particulate Coll. (g)	Volume Samp. (m ³)	Part. Load. (mg/m ³)
MM5-1 (TB2)	5/11/93	0.13023	2.982	43.67
MM5-2 (TB3)	5/13/93	0.65767	4.792	137.24
MM5-3 (TB4)	5/17/93	0.66563	6.986	95.28
MM5-4 (TB5)	5/18/93	0.08536	4.915	17.37
MM5-5 (TB8)	5/21/93	0.64017	4.815	132.95
MM5-6 (TB9)	5/25/93	1.46328	5.126	285.46
MMT-1 (TB6)	5/19/93	0.5007	4.957	101.01
MMT-2 (TB7)	5/20/93	0.0197	4.755	4.14

Table F-4. Residuals from COEMISFAC regression models.

Run	Model-1	Model-2	Model-3
TB6	-0.207	-0.196	-0.343
TB7	0.163	0.156	-1.714
TB10	-0.070	-0.068	0.622
TB11	0.479	0.480	0.735
TB12	0.854	0.856	0.717
TB13	1.921	1.923	2.723
TB14	-0.870	-0.868	-1.210
TB15	-1.099	-1.099	-0.697
TB16	-0.493	-0.493	-0.933
TB17	-0.897	-0.897	-1.018
TB18	-0.581	-0.583	-0.828
TB19	0.198	0.196	-0.007
TB20	-0.004	-0.006	1.663
TB21	0.688	0.686	0.721
TB22	-0.639	-0.641	-0.610
TB23	-1.698	-1.694	-1.746
TB24	1.381	1.382	1.007
TB25	-0.813	-0.811	-1.279
TB26	1.381	1.382	2.582
TB27	-2.007	-2.010	0.330
TB28	-0.037	-0.040	-1.155
TB29	4.036	4.033	1.734
TB30	-0.485	-0.488	-1.295

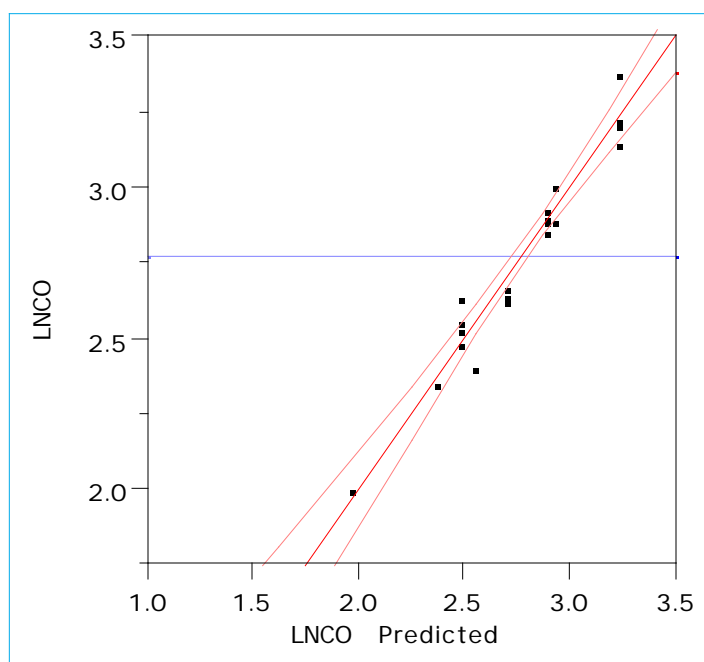


Figure F-1. CO Model 1; Predicted ln(COEMISFAC) vs. measured ln(COEMISFAC).

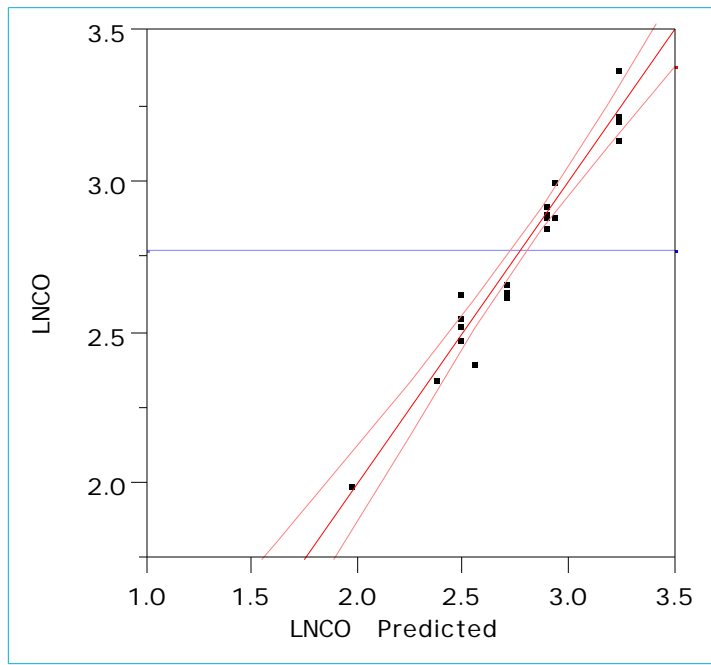


Figure F-2. CO Model 2; Predicted $\ln(\text{COEMISFAC})$ vs. measured $\ln(\text{COEMISFAC})$.

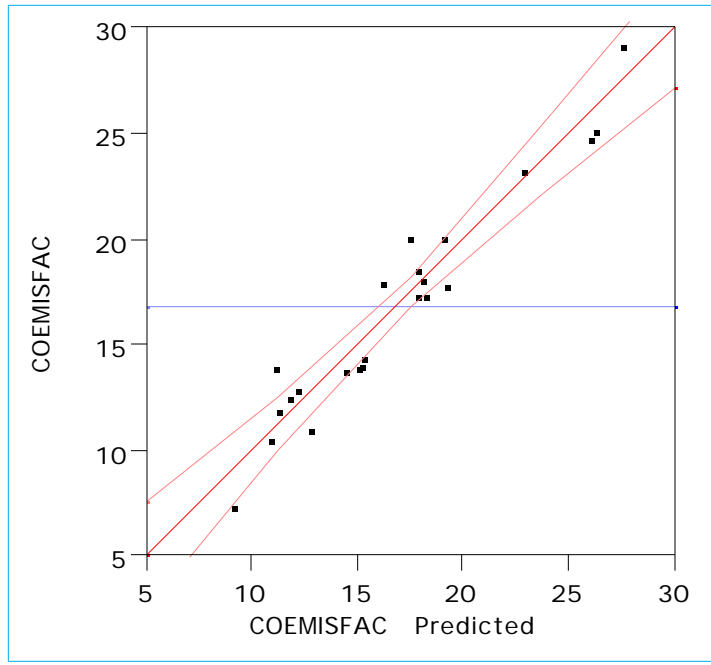


Figure F-3. CO Model 3; Predicted COEMISFAC vs. measured COEMISFAC .

Table F-5. Residuals (x 1000) from PAHEMISFAC regression models.

Run	Model-1	Model-2	Model-3
TB6	-1.802	-0.436	-0.367
TB7	0.169	0.138	0.512
TB10	-0.340	-0.360	-0.181
TB11	0.218	-0.044	-0.279
TB12	-0.360	-0.612	-0.271
TB13	0.139	-0.090	0.497
TB14	-0.923	0.133	-0.632
TB15	0.588	1.040	0.107
TB16	1.049	1.137	0.243
TB17	-0.525	-0.318	-1.145
TB18	0.415	0.857	0.810
TB19	-0.766	-0.444	0.659
TB20	3.105	2.088	1.023
TB21	-1.220	-0.546	-0.252
TB22	1.934	-1.106	-0.645
TB23	0.457	0.317	-0.945
TB24	0.776	3.357	2.065
TB25	-1.010	-1.937	-0.284
TB26	-0.670	1.501	0.708
TB27	-0.358	-3.030	-1.412
TB28	2.676	-0.054	1.046
TB29	-1.076	1.492	-0.414
TB30	-1.023	-2.285	-0.844

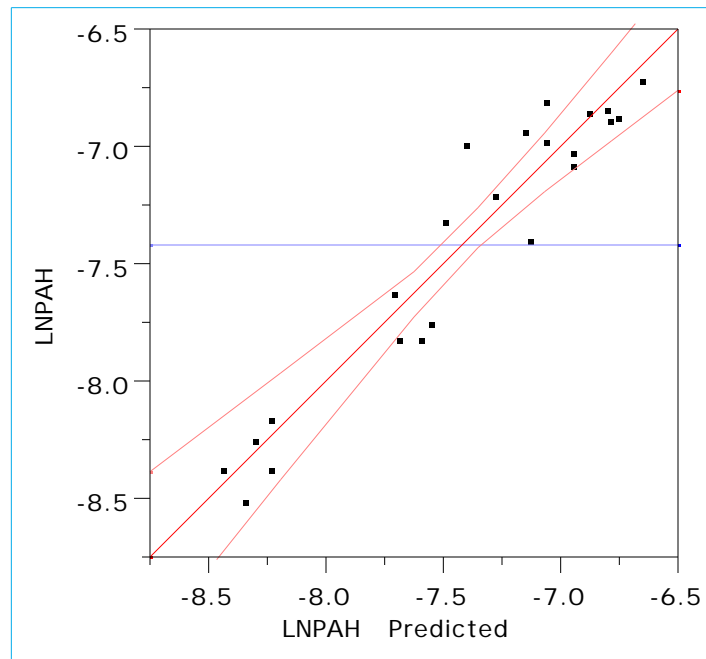


Figure F-4. PAH Model 1; Predicted ln(PAHEMISFAC) vs. measured ln(PAHEMISFAC).

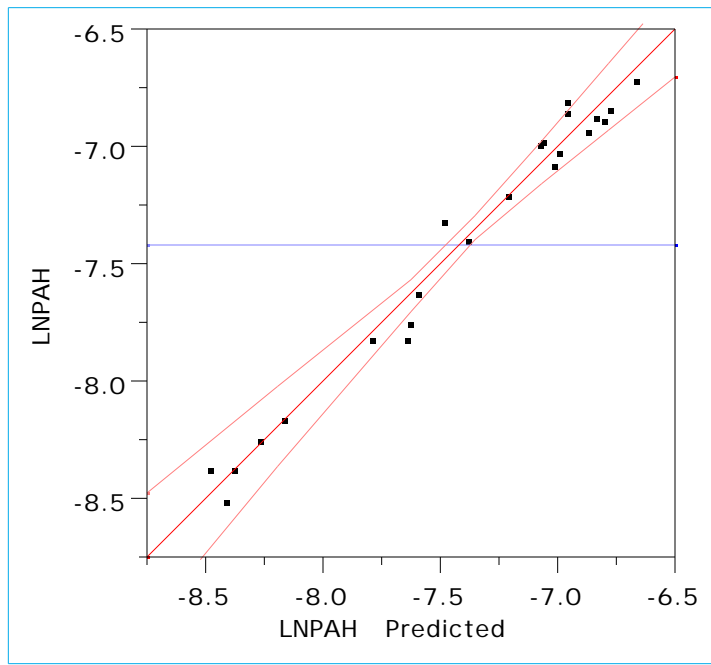


Figure F-5. PAH Model 2; Predicted ln(PAHEMISFAC) vs. measured ln(PAHEMISFAC).

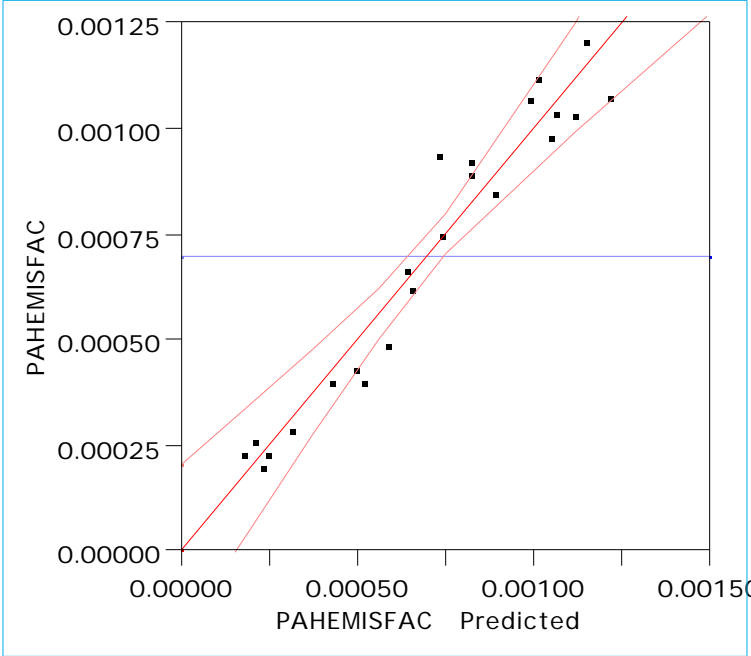


Figure F-6. PAH Model 3; Predicted PAHEMISFAC vs. measured PAHEMISFAC.

TECHNICAL REPORT DATA		
Please read Instructions on the reverse before completing)		
1. REPORT NO. EPA-600/R-94-070	2.	3. RECIPIENT'S ACCESSION NO.
4. TITLE AND SUBTITLE Pilot-scale Evaluation of the Potential for Emissions of Hazardous Air Pollutants from Combustion of Tire-derived Fuel	5. REPORT DATE April 1994	
	6. PERFORMING ORGANIZATION CODE	
7. AUTHOR(S) Paul M. Lemieux	8. PERFORMING ORGANIZATION REPORT NO.	
9. PERFORMING ORGANIZATION NAME AND ADDRESS See Block 12	10. PROGRAM ELEMENT NO.	
	11. CONTRACT/GRANT NO. 68-DO-0141 (Acurex) and CR814945-01-0 (Univ. of Arkansas)	
12. SPONSORING AGENCY NAME AND ADDRESS EPA, Office of Research and Development Air and Energy Engineering Research Laboratory Research Triangle Park, NC 27711	13. TYPE OF REPORT AND PERIOD COVERED Final; 2/92 - 10/93	
	14. SPONSORING AGENCY CODE EPA/600/13	
15. SUPPLEMENTARY NOTES AEERL project officer is Paul M. Lemieux, Mail Drop 65, 919/541-0962		
16. ABSTRACT <p>The report gives results of experiments in a 73-kW (250,000) Btu/hr rotary kiln incinerator simulator to examine and characterize emissions from incineration of scrap tire material. The purposes of the project were to: (1) generate a profile of target analytes for full-scale stack sampling, not statistically defensible emission factors for the controlled combustion of scrap tire material; and (2) where possible, give insight into the technical issues and fundamental phenomena related to controlled combustion of scrap tires. Wire-free crumb rubber, sized at < 0.64 cm (<1/4 in.), was combusted at two feed rates, two temperatures, and three kiln oxygen (O₂) concentrations. Along with continuous emission monitoring for O₂, carbon dioxide, carbon monoxide, nitric oxide, sulfur dioxide, and total hydrocarbons, samples were taken to examine volatile and semi-volatile organics, polychlorinated p-dibenzodioxins and dibenzofurans, and metal aerosols. In addition, a continuous polycyclic aromatic hydrocarbon analyzer was used in all tests. Samples were analyzed with emphasis on the 189 hazardous air pollutants listed in the 1990 Clean Air Act Amendments, but other compounds were also identified, where possible. Overall, except for zinc, potential emissions from tire-derived fuel do not appear to be significantly different from emissions from conventional fossil fuel combustion in a well-designed and well-operated combustion device.</p>		
17. KEY WORDS AND DOCUMENT ANALYSIS		
a. DESCRIPTORS	b. IDENTIFIERS/OPEN ENDED TERMS	c. COSATI Field/Group
Pollution Tires Fuels Combustion Incinerators Emission	Toxicity Pollution Control Stationary Sources	13B 06T 13F 21D 21B
18. DISTRIBUTION STATEMENT Release to Public	19. SECURITY CLASS (<i>This Report</i>) Unclassified	21. NO. OF PAGES 134
	20. SECURITY CLASS (<i>This Page</i>) Unclassified	22. PRICE